

Accepted Manuscript

Oxadiazole-substituted naphtho[2,3-*b*]thiophene-4,9-diones as potent inhibitors of keratinocyte hyperproliferation. Structure–activity relationships of the tricyclic quinone skeleton and the oxadiazole substituent

Atila Basoglu, Simone Dirkmann, Nader Zahedi Golpayegani, Silke Vortherms, Jan Tentrop, Dominica Nowottnik, Helge Prinz, Roland Fröhlich, Klaus Müller

PII: S0223-5234(17)30252-0

DOI: [10.1016/j.ejmech.2017.03.084](https://doi.org/10.1016/j.ejmech.2017.03.084)

Reference: EJMECH 9344

To appear in: *European Journal of Medicinal Chemistry*

Received Date: 11 January 2017

Revised Date: 1 March 2017

Accepted Date: 31 March 2017

Please cite this article as: A. Basoglu, S. Dirkmann, N.Z. Golpayegani, S. Vortherms, J. Tentrop, D. Nowottnik, H. Prinz, R. Fröhlich, K. Müller, Oxadiazole-substituted naphtho[2,3-*b*]thiophene-4,9-diones as potent inhibitors of keratinocyte hyperproliferation. Structure–activity relationships of the tricyclic quinone skeleton and the oxadiazole substituent, *European Journal of Medicinal Chemistry* (2017), doi: 10.1016/j.ejmech.2017.03.084.

This is a PDF file of an unedited manuscript that has been accepted for publication. As a service to our customers we are providing this early version of the manuscript. The manuscript will undergo copyediting, typesetting, and review of the resulting proof before it is published in its final form. Please note that during the production process errors may be discovered which could affect the content, and all legal disclaimers that apply to the journal pertain.

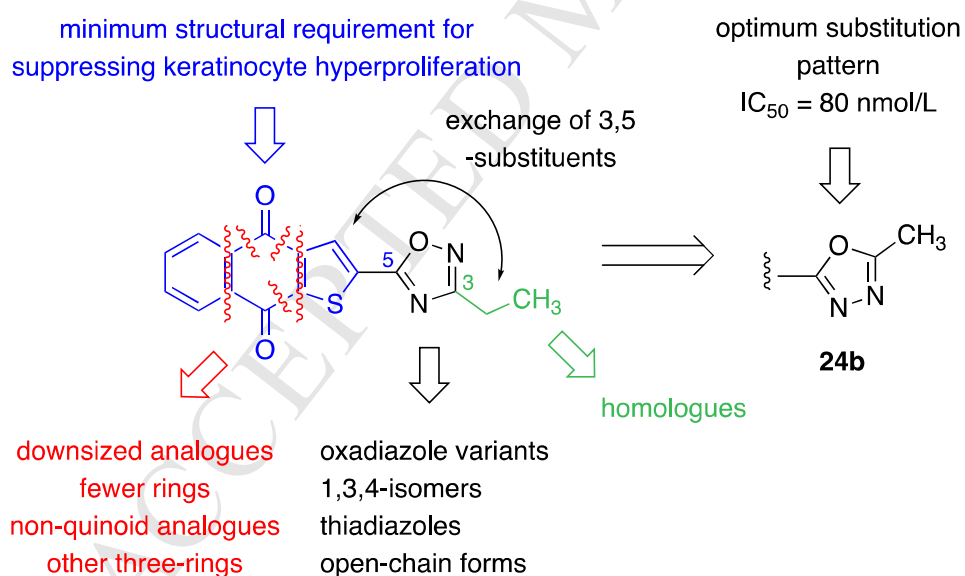


Oxadiazole-substituted naphtho[2,3-*b*]thiophene-4,9-diones as potent inhibitors of keratinocyte hyperproliferation. Structure–activity relationships of the tricyclic quinone skeleton and the oxadiazole substituent

Atila Basoglu,[†] Simone Dirkmann,[†] Nader Zahedi Golpayegani,[†] Silke Vortherms,[†] Jan Tentrop,[†] Dominica Nowottnik,[†] Helge Prinz,[†] Roland Fröhlich,[‡] and Klaus Müller^{*·†}

[†] *Institute of Pharmaceutical and Medicinal Chemistry, PharmaCampus, Westphalian Wilhelms University, Corrensstraße 48, D-48149 Münster, Germany*

[‡] *Organic Chemistry Institute, Westphalian Wilhelms University, Corrensstraße 40, D-48149 Münster, Germany*



Oxadiazole-substituted naphtho[2,3-*b*]thiophene-4,9-diones as potent inhibitors of keratinocyte hyperproliferation. Structure–activity relationships of the tricyclic quinone skeleton and the oxadiazole substituent

Atila Basoglu,[†] Simone Dirkmann,[†] Nader Zahedi Golpayegani,[†] Silke Vortherms,[†] Jan Tentrop,[†] Dominica Nowotnik,[†] Helge Prinz,[†] Roland Fröhlich,[‡] and Klaus Müller^{*†}

[†] *Institute of Pharmaceutical and Medicinal Chemistry, PharmaCampus, Westphalian Wilhelms University, Corrensstraße 48, D-48149 Münster, Germany*

[‡] *Organic Chemistry Institute, Westphalian Wilhelms University, Corrensstraße 40, D-48149 Münster, Germany*

* Corresponding author: Tel.: +49 251 833 3324

E-mail address: kmuller@uni-muenster.de

Abstract

Novel analogues of oxadiazole-substituted naphtho[2,3-*b*]thiophene-4,9-diones were synthesized in which the tricyclic quinone skeleton was systematically replaced with simpler moieties, such as structures with fewer rings and open-chain forms, while the oxadiazole ring was maintained. In addition, variants of the original 1,2,4-oxadiazole ring were explored. Overall, the complete three-ring quinone was essential for potent suppression of human keratinocyte hyperproliferation, whereas analogous anthraquinones were inactive. Also, the oxadiazole ring per se was not sufficient to elicit activity. However, rearrangement of the heteroatom positions in the oxadiazole ring resulted in highly potent inhibitors with compound **24b** being the most potent analogue of this series showing an IC₅₀ in the nanomolar range. Furthermore, experiments in isolated enzymatic assays as well as in the keratinocyte-based hyperproliferation assay did not support a major role of redox cycling in the mode of action of the compounds.

Keywords:

Antiproliferative Activity

HaCaT Cells

Quinone

Redox Activation

Superoxide Radical

Abbreviations:

7-AAD, 7-aminoactinomycin D; CPR, NADPH-cytochrome P450 oxidoreductase; DCC, *N,N'*-dicyclohexylcarbodiimide; DHE, dihydroethidium; DMAP, 4-(dimethylamino)pyridine; DTPA, diethylenetriaminepentaacetic acid; NQO-1, NAD(P)H:quinone oxidoreductase 1; ROS, reactive oxygen species; rt, room temperature; SAR, structure–activity relationship; SOD, superoxide dismutase.

1. Introduction

Naphthoquinones constitute a class of naturally occurring compounds found in animals, plants and microorganisms [1]. Due to their biological and structural properties they are regarded as privileged structures in Medicinal Chemistry [2], and because of their demonstrated activity particularly against cancer cells these agents have been the subject of intensive research [3,4]. The exact molecular mechanism by which naphthoquinones exert their biological action still needs to be elucidated. At least in part, the leading theory holds that the quinone moiety reacts with two major enzymes such as NADPH-cytochrome P-450 oxidoreductase (CPR) and NAD(P)H:quinone oxidoreductase 1 (NQO-1), leading to redox cycling between the quinone and the semiquinone radical or hydroquinone forms (Fig. 1), thereby generating superoxide and even more reactive oxygen species (ROS) derived therefrom that could react with biological targets [5-11].

Prominent examples of bioactive naphthoquinones (Fig. 2) include ortho-quinoid β -lapachone (**1**) and the linearly anellated naphtho[2,3-*b*]furan-4,9-diones **2** (napabucasin) and **3**, which were isolated from the heartwood of the lapacho (*Tabebuia*) tree of the Bignoniaceae family together with a variety of other naphthoquinones and anthraquinones [12-14]. The inner bark, commonly known as “pau-d’arco”, is used as an analgesic, an antiinflammatory, and an antineoplastic by the native people in South America [15,16]. The biological significance of these quinones in cancer therapy has stimulated enormous research interest in this class of compounds [17-22]. Furthermore, we have previously reported that the lapacho tree provided some naphthoquinones with comparable activity against the growth of human keratinocytes relative to the antipsoriatic drug anthralin (**4**, Fig. 2) [23].

In our continuous interest in tricyclic antiproliferative agents such as anthracenones [24] naphtho[2,3-*b*]thiophen-4(9*H*)-ones [25], acridones [26], phenoxazines and phenothiazines [27] we prepared novel analogues of napabucasin (**2**) and studied the influence of side chain modification on

the potency of these agents to suppress keratinocyte hyperproliferation [28]. Such a feature may be useful in the treatment of hyperproliferative skin disorders such as psoriasis, which is mainly characterized by excessive growth of keratinocytes [29]. In a subsequent study, we reported the synthesis and structure–activity relationships (SAR) for a series of compounds in which the furano-oxygen of the parent naphtho[2,3-*b*]furan-4,9-dione core was replaced by other heteroatoms [30]. Of these heterocyclic ring variants, the 8-hydroxynaphtho[2,3-*b*]thiophene-4,9-dione analogue bearing an oxadiazole ring on the 2-position of the tricyclic skeleton (**5**, Fig. 2) was the most potent inhibitor of keratinocyte hyperproliferation [30]. In this context, it is of interest to note that several compounds possessing an oxadiazole moiety have recently been reported as antiproliferative agents [31-35].

To further explore structure–activity relationships for the class of linearly anellated tricyclic quinones, we have now focused on identifying the minimum structural requirements for inhibitory action against keratinocyte hyperproliferation on the one hand, and, on the other, elucidating the role of the 2-oxadiazole substituent. Toward this goal, we compared the inhibitory potential of certain structural analogues in which the tricyclic quinone skeleton of naphtho[2,3-*b*]thiophene-4,9-dione **6** (Fig. 2) has been systematically replaced with simpler moieties while the 1,2,4-oxadiazole fragment was kept unchanged. We also report on the modification of the 1,2,4-oxadiazole ring of **6**, which resulted in a highly potent inhibitor of keratinocyte hyperproliferation. The biological testing procedures applied in this study were similar to those in our earlier work [28,30].

2. Chemistry

The syntheses of the desired substitution patterns and oxadiazole ring variants are shown in Schemes 1-6. Scheme 1 shows the preparation of **6** and its modified analogues **13a–13c** and **13l**. The required electron-rich 4,9-dimethoxynaphtho[2,3-*b*]thiophene (**8**) was prepared from unsubstituted quinone skeleton **7** by reductive methylation with sodium dithionite and dimethyl sulfate in the presence of tetrabutylammonium bromide. Regioselective 2-lithiation of the thiophene ring followed by carboxylation with dry ice yielded the activated carboxylic acid **9a**, which was then converted to 1,2,4-oxadiazole **13a** with *N*-hydroxypropionamidine in a one-pot reaction [36]. Oxidative deprotection of **13a** with diammonium cerium(IV) nitrate afforded quinone **6**. In a similar fashion, naphthothiophens **13b** and **13c**, which lack the methoxy group at the 9-position or both methoxy groups at the 4,9-positions, respectively, were prepared from precursors **10** and **12**. 4-Hydroxy analogue **13l** was obtained from its methoxy precursor **13b** by ether cleavage with boron tribromide.

The preparation of analogous compounds **13d–13f** and **13m–13u** (Charts 1, 3 and 4), in which the tricyclic quinoid system was downsized or replaced by other moieties, was also accomplished by reaction of the activated carboxylic acids and *N*-hydroxypropionamidine (Scheme 2). The requisite carboxylic acids were prepared as described in the Supplementary content or according to literature methods. Analogues comparable to **6** in which the 1,2,4-oxadiazole was appended to a quinone moiety (**13g–13k**, Chart 2) were obtained from their corresponding para-dimethoxy aromatic precursors by oxidative demethylation as described above.

Scheme 3 outlines the synthesis of 5-ethyl-1,2,4-oxadiazole **19**, which is a substitution isomer of **6** where the 3,5-substituents at the oxadiazole ring have been exchanged with each other. Carbaldehyde **14** was transformed into the corresponding oxime **15** and dehydrated to nitrile **16**, which upon addition of hydroxylamine furnished amidoxime **17**. Ring closure with activated propionic acid in a one-pot reaction in pyridine following the method of Borg et al. [36] provided

oxadiazole **18**, which was then converted to the quinoid structure **19**. In a similar fashion, anthraquinone-substituted oxadiazole **19a** (Table 1), a substitution isomer of **13g**, was prepared from 9,10-dimethoxyanthracene-2-carbaldehyde (see Supplementary content).

A series of related 1,3,4-oxadiazoles and 1,3,4-thiadiazoles was synthesized as shown in Scheme 4. Steglich esterification [37] of carboxylic acid **9a**, followed by reaction of methyl ester **20** with hydrazine, provided hydrazide **21**. Condensation of **21** and appropriate commercially available orthoesters under microwave irradiation, which was catalyzed by solid supported Nafion[®]NR50 according to the method of Polshettiwar [38], afforded 1,3,4-oxadiazoles **22a–22e**. Attempts to extend this method for the preparation of 1,3,4-thiadiazole analogues **23a–23c** using phosphorus pentasulfide in aluminum oxide as thionating agent were met with difficulty. While trimethyl orthoformate yielded **23a** as the main product, analysis of the reaction products showed that other orthoesters led predominantly to the formation of oxadiazoles, indicative of incomplete thionation of the hydrazides. To circumvent this problem, hydrazide **21** was refluxed with the thionating agent in acetonitrile. To our surprise, the expected thiohydrazide was already cyclized to **23b** under these conditions, suggesting that acetonitrile reacted with the thiohydrazide followed by cyclization to form the 5-methyl-1,3,4-thiadiazole ring. When acetonitrile was replaced by dioxane and triethyl orthopropionate, moderate yields of the 5-ethyl-1,3,4-thiadiazole **23c** were obtained. In the final step, deprotection of the hydroquinone ethers **22a–22e** and **23a–23c** gave the corresponding target quinones **24a–24e** and **25a–25c**, respectively.

The syntheses of the 2-substituted open-chain analogues of oxadiazole **6** are shown in Scheme 5. The Tanaka procedure [39] was used to prepare the key intermediates **9a** and **14**, which involved metalation of **8** with *n*-butyllithium and quenching the resulting anion with dry ice or *N,N*-dimethylformamide, respectively. Nitrile **16** was obtained from **14**, whereas ester **20** and hydrazide **21** were obtained from **9a** as described in Schemes 3 and 4, respectively. Reaction of nitrile **16** with

sodium azide in DMF resulted in tetrazole **26**. The α,β -unsaturated carbonyl compounds **27** and **28** were prepared from carbaldehyde **14** in an aldol reaction. The final deprotection step yielded analogues **29–36**. Hydrazones **37** and **38** were directly prepared from deprotected aldehyde **32** and the appropriate hydrazines.

Finally, nitration of naphtho[2,3-*b*]thiophene-4,9-dione (**7**) according to a literature procedure [40] gave rise to an isomeric mixture of the 2- and 3-nitro analogues (Scheme 6), which were separable by chromatography. NMR data did not allow unambiguous spectral assignment of the position of the nitro group. However, X-ray crystal structures of **39a** and **39b** (see Supplementary content for details) unequivocally confirmed the position of the nitro substituent for both isomers. The 2-nitro isomer **39a** was then reduced with sodium dithionite to the 2-amino analogue **40**. Schotten-Baumann reaction [41] with aliphatic acid chlorides in pyridine or aromatic acid chlorides in dichloromethane provided the aliphatic amides **41a–41c** and aromatic amides **41d** and **41e**, respectively (Scheme 6).

3. Biological evaluation and discussion

3.1. *Suppression of keratinocyte hyperproliferation and SAR for the three-ring skeleton and the oxadiazole ring*

The ability of the compounds to suppress keratinocyte hyperproliferation was measured using a spontaneously transformed human keratinocyte (HaCaT) cell line [42] which displays a keratinization pattern typical of that seen in the psoriatic epidermis. These adherent cells grow as a layer and are very good mimics for hyperproliferative skin, making them a highly relevant model for psoriasis and for the preclinical evaluation of potential antipsoriatic agents [43]. The data for the

antipsoriatic agent anthralin (**4**) and the naturally occurring β -lapachone (**1**) obtained in this assay are shown for comparison (Table 1). IC_{50} values for antihyperproliferative activity of the novel compounds are recorded in Charts 1–4 and Tables 1 and 2.

The compounds prepared were designed to answer two questions concerning SAR for inhibitory activity against keratinocyte hyperproliferation among the 2-substituted naphtho[2,3-*b*]thiophene-4,9-diones. For this purpose, three series of compounds were studied. In order to more closely delineate the minimum requirements for activity, we have prepared analogues of the most active representative, 2-oxadiazole-substituted **5**, in which drastic alterations of the original tricyclic quinone structure were made to see whether compounds with fewer rings and open-chain forms are still active (Charts 1–4). As the tricyclic skeleton contains the quinone motif, it may lead to redox reaction and nonspecific interaction with sulfur nucleophiles such as cysteine present in proteins [44]. The latter feature, however, can be ignored in the case of the heterocycle-fused naphthoquinones. As compared to menadione, which has a nonfused quinone ring, these agents do not have an unsubstituted β -carbon open to nucleophilic attack and cannot form adducts as a Michael acceptor. Nonetheless, they are redox active by virtue of their quinone moiety [28,30]. To shed some more light on a possible nonspecific contribution of the quinone moiety in the context of the compounds under study, we also included two anthraquinone-analogous and three nonfused naphthoquinone-analogous structures of naphtho[2,3-*b*]thiophene-4,9-dione **6** (**13g–13k**, Chart 2, **19a**, Table 1).

Compounds depicted in Tables 1 and 2, however, explore further modifications of the 2-oxadiazole substituent of **5** and are either oxadiazole ring variants (Table 1) or open-chain analogues (Table 2). The decision to remove the 8-hydroxy group in **5** is based on an observation from our earlier study that this group is associated with release of larger amounts of lactate dehydrogenase into the culture medium and responsible for membrane-damaging effects [30]. As recently reported, this drawback

can be eliminated by substitution with a chloro or an hydrogen atom, even though the 8-chloro-substituted compound was somewhat less potent [45]. As a compromise, 8-unsubstituted **6**, a closely related congener of **5**, was chosen for further SAR studies.

3.1.1. Simplification of the tricyclic quinone skeleton

Some of the para-dimethoxy substituted precursors of the quinones were tested for inhibition of keratinocyte hyperproliferation, along with unsubstituted three or two ring-fused analogues (**13a–13f**, Chart 1). None of these are active except for the 4,9-dimethoxynaphthothiophene derivative **13a**, which, however, is almost 20-fold less potent than **6**. Chart 2 reveals that a quinone structure alone is not sufficient for potency. Those analogues in which either the fused phenyl (**13k**) or thiophene ring (**13i**) of **6** was omitted display only moderate activity, whereas an anthraquinone-based analogue (**13g**) of **6** as well as naphthoquinone **13h**, where the oxadiazole ring is directly attached to the quinone ring, are both inactive (defined as an IC_{50} of $> 30 \mu\text{mol/L}$). In the tricyclic compounds of Chart 3, either one of the carbonyl oxygen atoms was removed (**13l**, **13p**) or one carbonyl group of the quinone was replaced with an oxygen (**13m**, **13o**) or a sulfur atom (**13n**). While in the latter cases, as documented by xanthenes **13m** and **13o** as well as thioxanthone **13n**, activity is lost, anthrone-type agents **13l** and **13p** are about 20-fold less potent than lapacho analogue **6**. In addition, the compounds of Chart 4 were prepared to study the further dissection of **6** into simpler analogues such as **13q**, which completely lacks the 4-carbonyl group, **13s**, which retains the thiophene ring together with the original 4-carbonyl group, **13u** with only the thiophene ring left at the oxadiazole, or the corresponding phenyl analogues of the last-mentioned compounds, i. e. **13r** and **13t**, respectively. Taken together, all these modifications of the tricyclic quinone structure of **6** are accompanied by loss of activity or reduced potency against keratinocyte hyperproliferation. Accordingly, the results from these downsized or modified structures lead to the

conclusion that the intact tricyclic molecular skeleton is the essential moiety required for antihyperproliferative activity. Our results also question whether an oxadiazole moiety per se is sufficient to elicit an antiproliferative action. Initially, the oxadiazole ring was considered to be a bioisostere for esters or amides [46]. More recently, a body of evidence has emerged that suggests a role for a 1,2,4- or a 1,3,4-oxadiazole ring system in antiproliferative active agents [31-34], which is not supported by this study, at least with respect to the action against keratinocyte hyperproliferation.

With respect to the quinone motif, the results obtained with naphthoquinones **13h–13k** (Chart 2), menadione (Table 1), anthraquinones **13g** (Chart 2) and **19a** (Table 1) clearly show that the potent action of the linearly anellated naphtho[2,3-*b*]thiophene-4,9-diones against keratinocyte hyperproliferation is not simply the consequence of their quinone structure, since in particular both anthraquinones in which the anellated thiophene ring is replaced by a phenyl ring are inactive.

3.1.2. Oxadiazole ring variants

In the following compound series, variants of the original 3-ethyl-1,2,4-oxadiazole ring have been explored, and data for suppression of keratinocyte hyperproliferation are collected in Table 1. When the tricyclic skeleton in position 5 of the 1,2,4-oxadiazole of **6** has been switched with the ethyl group of the 3-position, as exemplified by its isomer **19**, potency is still in the low micromolar range, but somewhat reduced as compared to **6** (IC₅₀ of 0.58 μmol/L vs. 0.36 μmol/L). However, when the naphtho[2,3-*b*]thiophene-4,9-dione moiety of **19** has been exchanged for an anthraquinone core (**19a**), activity is lost, confirming the results obtained with anthraquinone **13g** (Chart 2), which is an isomer of **19a**. By contrast, modification of the heteroatom positions in the oxadiazole ring from a 1,2,4- to a 1,3,4-arrangement resulted in highly potent inhibitors with IC₅₀ values in the

submicromolar range. The corresponding 1,3,4-isomer **24c** was more potent than 1,2,4-arranged **6** ($IC_{50} = 0.15 \mu\text{mol/L}$ vs. $IC_{50} = 0.36 \mu\text{mol/L}$).

Compounds **24a–24e** explore the consequences of varying the length of the 5-alkyl chain on the 1,3,4-oxadiazole ring. Extending the chain of the original ethyl group of the 1,3,4-isomer **24c** by two carbon atoms to give butyl substituted **24d** reduced potency. On the other hand, when the chain was shortened by one carbon atom to provide the methyl substituted **24b**, potency was improved, but did not show further improvement when the methyl group was removed as in **24a**. Replacement of the alkyl group with a phenyl ring gave an inactive compound (**24e**). By comparing the homologous series of 5-alkyl-1,3,4-oxadiazoles **24a–24e**, peak activity against keratinocyte hyperproliferation ($IC_{50} = 0.08 \mu\text{mol/L}$) is shown by **24b**, which is the most potent compound seen so far under our assay conditions. Exchanging the 1,3,4-oxadiazole for a 1,3,4-thiadiazole ring resulted in analogues **25a–25c**. The inhibitory potency determined for these compounds clearly suggests that the oxadiazole is preferred relative to the thiadiazole, i. e. **24b**, IC_{50} of $0.08 \mu\text{mol/L}$ compared to **25b**, IC_{50} of $3.70 \mu\text{mol/L}$.

3.1.3. Open-chain analogues

A third series of compounds was prepared for comparison with **6** and to evaluate SAR for open side-chain substituents. A number of carbonyl-containing groups such as esters and amides that would be mimicked by the oxadiazole ring have been explored at the 2-position of the naphtho[2,3-*b*]thiophene-4,9-dione (Table 2). There was a clear distinction in hyperproliferation inhibitory properties between the free acid **29** and its corresponding methyl ester **30**. While the free acid is not active and may not be able to cross the keratinocyte membrane, ester **30** is a potent inhibitor of keratinocyte hyperproliferation, with an IC_{50} of $0.71 \mu\text{M}$ in the same order of magnitude to those of anthralin and β -lapachone.

Also, when the carboxylic acid group of **29** was replaced by a tetrazole-5-yl group (**34**), which was used as a nonclassical bioisosteric replacement, as it has comparable acidity to that observed for the carboxylic acids while being about ten times more lipophilic [47], activity was not apparent in this assay. As with ester **30**, hydrazone **31** and aldehyde **32** display activity, though slightly reduced but 3–5-fold better than the 2-methyl analogue **43**. Comparing chalcones **35** and **36** as well as hydrazones **37** and **38** with **6** shows that opening the oxadiazole ring results in the loss of inhibitory activity for each analogue. This is also the case for compound **40** having a 2-amino group. Activity is regained by converting the amine into amides **41a–41e**. Within this homologous series of small and branched alkyl groups (**41a–41c**), these compounds are active in the micromolar range, but 9–27-fold less potent than oxadiazole **6**. Benzamides **41d** and **41e** are somewhat more potent than the aliphatic amides, and their potency is similar to that of the two nitro derivatives **39a** and **39b**. The most potent compounds of the open-chain analogues are nitrile **33** and the 2-acetylated **42** (IC_{50} of 0.44 $\mu\text{mol/L}$), which is the sulfur analogue of the original lapacho constituent napabucasin (**2**), and these compounds are essentially equipotent. Altogether, smaller groups at the 2-position may be advantageous for potency, and there also seems to be a requirement for an electron-withdrawing group.

3.2. *Enzymatic redox activation*

As previously reported [28], selected compounds were subjected to redox cycling experiments where superoxide generation was evaluated both by the CPR- and NQO-1-catalyzed one- and two-electron reduction, and this was also confirmed in keratinocyte-based assays. Typically, the quinones are reduced in two sequential reactions to generate hydroquinones via semiquinone radicals that can react back to the parent compounds, thus perpetuating a redox cycle (Fig. 1). As a result, these reduced forms of the quinones rapidly produce superoxide as the initial species by

electron transfer to molecular oxygen. Dismutation of superoxide yields hydrogen peroxide, which can react with trace amounts of ferrous ions to form even more reactive species, such as hydroxyl radicals. If accumulation of reactive oxygen species overwhelms the antioxidant capacity of the cell, this can lead to oxidative stress [48], failure of normal cellular functions and even cell death [49]. The ability of the naphtho[2,3-*b*]thiophene-4,9-diones to stimulate superoxide generation was determined as described [28], and the results are presented in Table 3. The known redox cyclers menadione [50,51] (2-methylnaphthalene-1,4-dione) served as a positive control.

All the tested compounds were significant generators of superoxide in the one-electron reduction assay catalyzed by human recombinant CPR, and except for the basic structure **7**, also in the two-electron reduction by human recombinant NQO-1, though the contribution of the latter enzyme was somewhat less pronounced. The rates of superoxide generated by the lapacho compounds reflect an efficient interaction of their corresponding semiquinone radicals with molecular oxygen resulting in redox cycling and concomitant superoxide production. In contrast to the other agents tested, 2-nitro substituted **39a** was also an excellent substrate for NQO-1 and generated the highest amount of superoxide compared to other functional groups such as amino (**40**), acetyl (**42**), or methyl (**43**) at C-2 of the tricyclic quinone structure. This is not surprising, as in addition to quinones, NQO-1 is capable of catalyzing two-electron reduction of a wide variety of functional groups such as aromatic nitro compounds and can even catalyze four-electron reduction of the nitro group [52]. 2-Nitro-substituted **39a** was actually synthesized to study the effect of an additional structural feature in the molecule capable of redox cycling. Such a strategy has very recently been applied successfully to the design and synthesis of quinone-based triazoles possessing a second redox center [53].

3.3. *Superoxide generation in keratinocytes*

The amount of superoxide production was also directly determined in a keratinocyte-based assay under the conditions comparable to that of the hyperproliferation model in HaCaT cells to confirm

that an excessive amount of superoxide by redox cycling of the quinones is generated within whole cells. The fluorescence intensity arising from the product of the reaction of superoxide with the fluorescent probe dihydroethidium (DHE) was monitored by flow cytometry [54]. The oxidized form, 2-hydroxyethidium (2-OH-E⁺), is a measure of intracellular superoxide generation and a specific marker for superoxide [55,56]. As a positive control in these experiments we have also employed menadione, for which DHE was used to detect intracellular superoxide generation after treatment of cells with this quinone [55,57].

In most cases, significantly increased superoxide generation following both acute and chronic treatment of HaCaT keratinocytes with the selected lapacho compounds was observed, as quantified by the mean fluorescence intensities (Table 4). When keratinocytes were pretreated with dicoumarol, a commonly used inhibitor of NQO-1 [50,58] that competes with NADH for binding and prevents reduction of quinones, superoxide generation by the lapacho analogues was still significant as compared to controls. Accordingly, inhibition of the NQO-1-promoted two-electron metabolism of the quinones in keratinocytes by dicoumarol may increase the accessibility of these agents for one-electron reduction by CPR, and nevertheless allow efficient redox cycling with concomitant superoxide release via this alternative pathway (Fig. 1). As a consequence, 2-OH-E⁺ fluorescence is still enhanced and points towards a predominant role of the CPR pathway under these conditions. This is in line with the observation that all quinones were also activated by CPR in the isolated enzyme assay (Table 3).

As expected, also in the cellular assay we observed that the nitro aromatic analogue **39a** produced higher amounts of superoxide than compounds with other substituents in the 2-position of the tricyclic quinone skeleton. This is consistent with the well-known concept that reduction of nitro aromatic compounds by NADH-enzymes is initiated by means of the addition of an electron to generate the corresponding nitro radical anions. In the presence of oxygen, the nitro radical anions can rapidly interfere with oxygen to regenerate the original nitro compounds and produce

superoxide [59]. Moreover, the situation with a nitro group is further complicated by the fact that its consecutive reduction involves a nitroso derivative, a nitroxyl radical and the hydroxylamino functionality which in turn may also undergo redox cycling via the nitroxyl radical to produce superoxide [60]. The possible consequences of oxidative stress [48] in human keratinocytes with respect to the potential therapeutic action of the naphtho[2,3-*b*]thiophene-4,9-diones in the treatment of hyperproliferative skin disorders such as psoriasis have been discussed in detail previously [28].

However, while there are clear SARs for the structural requirements of the compounds to inhibit keratinocyte hyperproliferation, their potential to redox cycle does not correlate with their ability to arrest or slow down cell proliferation events. Thus, the nitro aromatic compound **39a** was prepared to check the contribution of an additional redox center at the tricyclic skeleton, which is reflected by the highest amounts of superoxide generated in both enzymatic and cell-based assays, but this analogue shows only mediocre activity in the keratinocyte model. On the other hand, amino analogue **40**, which is completely inactive against keratinocyte hyperproliferation, produces rates of superoxide comparable to those of potent analogues such as **6** or **42**. Accordingly, our present data do not support a major role of redox cycling in the mode of action of the lapacho analogues.

3.4. *Detection of apoptotic cells using 7-aminoactinomycin D (7-AAD)*

Then, we examined apoptosis from FACS analysis of HaCaT cells using 7-AAD staining for quantification following treatment with the compounds for 18 h. Cells in the early phase of apoptosis stain positive for 7-AAD in flow cytometry, depending on the concentration of the fluorescent intercalator [61]. When HaCaT keratinocytes were examined after chronic treatment with representative lapacho analogues (5 $\mu\text{mol/L}$), induction of cell death was enhanced as compared to controls but not significant (Table 4). Interestingly, oxadiazole analogue **6** produced an exceptionally high level of apoptotic cells. Furthermore, cells could be substantially protected by

pretreatment of HaCaT keratinocytes with the NQO-1 inhibitor dicoumarol suggesting the involvement of this enzyme in the activation of this compound. Finally, relatively high levels of superoxide produced by the most potent superoxide generator of this series, analogue **39a**, did not correlate with the potency of this agent to trigger cell death after chronic treatment. Therefore, the crucial species responsible for the biological action of the compounds that can interact with cellular macromolecules such as DNA, lipids or proteins and ultimately cause apoptosis of the cell needs still to be identified.

4. Conclusions

In this SAR study of oxadiazole-substituted naphtho[2,3-*b*]thiophene-4,9-diones, the importance of the tricyclic quinone skeleton was explored through the stepwise degradation of this moiety while the oxadiazole ring was kept unchanged. However, removal of one of the anellated rings or modifications within the quinone moiety were poorly tolerated, leading to decreases or loss in potency, suggesting the need for an intact heterocycle-fused naphthoquinone, whereas an oxadiazole ring per se was not sufficient for activity.

On the basis of their inhibitory effects on HcCaT cell hyperproliferation, it was further revealed that the replacement of the 1,2,4-oxadiazole by a 1,3,4-oxadiazole ring in the structure of **6** improved its antihyperproliferative ability. Moreover, within this particular class, further modifications of the 5-alkyl side chain have marked effects on potency. As a result, a methyl substituent was highly beneficial and led to the identification of **24b**, which with an IC_{50} of 0.08 $\mu\text{mol/L}$ was the most potent inhibitor of keratinocyte hyperproliferation we have obtained under the assay conditions. These findings support further development of this class of compounds for psoriasis or epidermal hyperplasia resulting from other causes.

5. Experimental section

5.1. Chemistry

Melting points were determined with a Kofler melting point apparatus and are uncorrected. ^1H NMR (400 MHz, 600 MHz) and ^{13}C NMR (151 MHz, 100 MHz) spectra were recorded on a Varian Mercury 400 plus or an Agilent DD2 600 spectrometer, using tetramethylsilane as an internal standard. Fourier transform IR spectra were recorded on a Shimadzu spectrometer type Miracle 10 (attenuated total reflection, ATR) by applying ATR correction. Mass spectra (ESI or APCI) were recorded on a Finnigan MAT GCQ instrument (70 eV) or on a Bruker-Daltonics MicroTOF QII instrument. Chromatography refers to column chromatography, which was performed on silica gel (0.063–0.200 mm, 6 nm, Macherey-Nagel) with CH_2Cl_2 as the eluant unless otherwise stated. Yields have not been optimized. The purity of all tested compounds was $\geq 95\%$ as determined by analytical reversed-phase HPLC (Ultimate 3000, Thermo-Fisher) or elemental analyses.

5.1.1. General procedure for the oxidative demethylation of hydroquinone dimethyl ethers

5.1.1.1. 2-(3-Ethyl-1,2,4-oxadiazol-5-yl)naphtho[2,3-b]thiophene-4,9-dione (**6**)

To a suspension of **13a** (0.30 g, 0.88 mmol) in MeCN (8 mL) and water (1.5 mL) at 0 °C was added dropwise within 20 min $(\text{NH}_4)_2[\text{Ce}(\text{NO}_3)_6]$ (1.50 g, 2.74 mmol) in MeCN (2.5 mL) and water (2.5 mL) under vigorous stirring. The mixture was allowed to react for 30 min under the same conditions. Then it was poured onto ice-water (50 mL) and extracted with CH_2Cl_2 (3 \times 50 mL). The combined organic phase was washed with a saturated solution of NaCl (2 \times 50 mL), dried over

Na₂SO₄, then concentrated, and purified by chromatography to afford light yellow, felted needles; 89% yield; mp 182 °C; FTIR 1681, 1645 cm⁻¹; ¹H NMR (CDCl₃) δ 8.38 (s, 1H), 8.32–8.24 (m, 2H), 7.88–7.78 (m, 2H), 2.86 (q, *J* = 7.6 Hz, 2H), 1.40 (t, *J* = 7.6 Hz, 3H); ¹³C NMR (CDCl₃, 101 MHz) δ 178.70, 178.20, 172.93, 169.79, 148.61, 143.18, 134.72, 134.38, 133.63, 133.39, 133.16, 129.89, 127.87, 127.44, 19.98, 11.59; MS (APCI) *m/z* 311.0418, calcd for C₁₆H₁₀N₂O₃S [M + H]⁺, 311.0485.

Analogously, target compounds **13g–13k**, **19**, **19a**, **24a–24e**, **25a–25c**, **29–36**, were prepared from the corresponding hydroquinone dimethyl ethers. See Supplementary content for details.

5.1.2 General procedure for the reductive methylation of quinones

5.1.2.1 4,9-Dimethoxynaphtho[2,3-*b*]thiophene (**8**)

To a solution of **7** [40] (5.00 g, 23.34 mmol) and tetrabutylammonium bromide (77 mg, 0.24 mmol) in dry THF (220 mL) under N₂ sodium dithionite (24.39 g, 140 mmol) in water (110 mL) was added dropwise. The mixture was vigorously stirred for 30 min and then treated with sodium hydroxide (28.04 g, 500 mmol) in water (110 mL). After 30 min it was cooled to 0 °C on an ice-bath, dimethyl sulfate (26.68 mL, 280 mmol) was added, and the mixture was then stirred for 2 h at 0 °C. Then it was allowed to warm to rt, stirred for an additional 2 h, and extracted with CH₂Cl₂ (3 × 200 mL). The combined organic phase was washed with water (3 × 200 mL), then with a saturated solution of NaCl (200 mL), dried over Na₂SO₄ and evaporated. The residue was purified by chromatography to afford yellow crystals; 83% yield; mp 156 °C; FTIR 1620, 1543 cm⁻¹; ¹H NMR (CDCl₃) δ 8.28 (dd, *J* = 6.2, 3.4 Hz, 1H), 8.22 (dd, *J* = 6.3, 3.4 Hz, 1H), 7.58 (d, *J* = 5.6 Hz, 1H), 7.55–7.48 (m, 2H), 7.43 (d, *J* = 5.6 Hz, 1H), 4.15 (s, 3H), 4.12 (s, 3H); MS (APCI) *m/z* 245.0639, calcd for C₁₄H₁₂O₂S [M + H]⁺, 245.0631.

5.1.3. 4,9-Dimethoxynaphtho[2,3-*b*]thiophene-2-carboxylic acid (**9a**)

To a mixture of *n*-butyllithium (1.6 mol/L, 5.40 mL, 8.60 mmol) in dry THF (8.5 mL) at -30 °C under N₂ was added dropwise a solution of **8** (1.07 g, 4.37 mmol) in dry THF (52 mL). The mixture was stirred and cooled to -78 °C, and then dry ice (22.00 g, 500 mmol) was added in portions under N₂. The mixture was stirred at -78 °C for 10 min, then allowed to warm to -20 °C within 30 min, and then poured into HCl (2 mol/L, 50 mL). The organic phase was separated and the aqueous phase extracted with ether (3 × 50 mL). The combined organic phase was extracted with NaOH (1 mol/L, 3 × 50 mL) and the aqueous phase acidified with HCl (2 mol/L) to pH 2. The carboxylic acid was extracted CH₂Cl₂ (3 × 200 mL), the organic phase dried over Na₂SO₄ and then the solvent removed *in vacuo* to afford an orange powder; 76% yield; mp 258 °C; FTIR 1681 (CO₂H) cm⁻¹; ¹H NMR (DMSO-*d*₆) δ 8.28–8.24 (m, 1H), 8.23 (s, 1H), 8.19–8.15 (m, 1H), 7.70–7.58 (m, 2H), 4.07 (s, 3H), 3.95 (s, 3H); MS (APCI) *m/z* 289.0535, calcd for C₁₅H₁₂O₄S [M + H]⁺, 289.0529.

Analogously, compounds **9b** and **9c** were prepared from **11** and **12** [62], respectively. See Supplementary content for details.

5.1.4. 4-Methoxynaphtho[2,3-*b*]thiophene (**11**)

To a mixture of anhydrous K₂CO₃ (1.87 g, 13.54 mmol) and methyl tosylate (4.52 g, 24.26 mmol, 3.66 mL) was added dropwise a suspension of **10** [63] (2.47 g, 12.31 mmol) in CH₃CN (150 mL). The mixture was stirred at 50 °C for 15 h. Then the solvent was evaporated, the residue treated with CH₂Cl₂ (100 mL), washed with HCl (2 mol/L, 2 × 50 mL), and then with a saturated solution of NaCl (2 × 50 mL). The organic phase was dried over Na₂SO₄, then the solvent was evaporated and the product purified by chromatography (cyclohexane/CH₂Cl₂, 3/1), to give a dark white powder; 73% yield; mp 71 °C; ¹H NMR (CDCl₃) δ 8.31–8.23 (m, 1H), 8.14 (s, 1H), 7.95–7.84 (m,

1H), 7.56 (d, $J = 5.7$ Hz, 1H), 7.49–7.47 (m, 1H), 7.47–7.44 (m, 1H), 7.43 (d, $J = 5.7$ Hz, 1H), 4.14 (s, 3H); MS (APCI) m/z 215.0528, calcd for $C_{13}H_{10}OS$ $[M + H]^+$, 215.0525.

5.1.5. 3-Ethyl-5-(4,9-dimethoxynaphtho[2,3-*b*]thiophen-2-yl)-1,2,4-oxadiazole (**13a**)

To a solution of **9a** (1.50 g, 5.72 mmol) in dry CH_2Cl_2 (30 mL) was added DCC (0.54 g, 2.60 mmol) under N_2 , and the mixture was stirred at 0 °C for 1 h. Then it was filtered and the solvent evaporated. The residue was treated with pyridine (30 mL), and a solution of *N*-hydroxypropionamidine (0.22 g, 2.51 mmol) in pyridine (6 mL) was added dropwise at rt. Then the mixture was refluxed for 3 h, cooled to rt, poured onto ice-water (200 mL), acidified with HCl (2 mol/L), and extracted with CH_2Cl_2 (3 × 50 mL). The combined organic phase was washed with water (2 × 200 mL) and dried over Na_2SO_4 . The solution was evaporated, and the product was purified by chromatography to afford yellow needles; 43% yield; mp 135 °C; FTIR 2843, 1597 cm^{-1} ; 1H NMR ($CDCl_3$) δ 8.39 (s, 1H), 8.31–8.20 (m, 2H), 7.61–7.51 (m, 2H), 4.18 (s, 3H), 4.16 (s, 3H), 2.88 (q, $J = 7.6$ Hz, 2H), 1.42 (t, $J = 7.6$ Hz, 3H); MS m/z 341.0888, calcd for $C_{18}H_{16}N_2O_3S$ $[M + H]^+$, 341.0954.

Analogously, compounds **13b–13f**, **13m–13o**, and **13q–13u** were prepared from the appropriate carboxylic acids. See Supplementary content for details.

5.1.6. 4,9-Dimethoxynaphtho[2,3-*b*]thiophene-2-carbaldehyde (**14**)

To a solution of **8** (3.68 g, 14.95 mmol) in dry THF (150 mL) at -30 °C under N_2 was added dropwise *n*-butyllithium (1.6 mol/L in THF, 19.63 mL, 31.40 mmol), and the mixture was stirred for 15 min. Then *N,N*-dimethylformamide (2.75 g, 2.89 mL, 37.64 mmol) in THF (30 mL) was added, and the mixture was stirred for an additional 3 h at rt. Then it was poured into ice-water (100 mL) and extracted with ether (3 × 50 mL). The combined organic phase was washed with a

saturated solution of NaCl (3 × 50 mL), dried over Na₂SO₄, concentrated and purified by chromatography to afford an orange-yellow powder; 70% yield; mp 169–170 °C; FTIR 1658 (CHO), 1581 cm⁻¹; ¹H NMR (CDCl₃) δ 10.09 (s, 1H), 8.25–8.13 (m, 3H), 7.56–7.44 (m, 2H), 4.12 (s, 3H), 4.07 (s, 3H); MS (APCI) *m/z* 273.0579, calcd for C₁₅H₁₂O₃S [M + H]⁺, 273.0580.

5.1.7. 4,9-Dimethoxynaphtho[2,3-*b*]thiophene-2-carbaldehyde oxime (**15**)

A solution of **14** (2.56 g, 9.39 mmol) in dry methanol (100 mL) was heated to reflux, and a solution of hydroxylamine hydrochloride (0.65 g, 9.39 mmol) and Na₂CO₃ (0.99 g, 9.39 mmol) in water (15 mL) was added. The mixture was refluxed for 3 h and then diluted with water (100 mL). To complete precipitation, it was kept at -20 °C for 12 h. Then the precipitate was collected by filtration and dried under vacuum to afford a yellow powder; 79% yield; mp 132 °C; FTIR 1651, 1603 cm⁻¹; ¹H NMR (CDCl₃) δ 8.35 (s, 1H), 8.20–8.10 (m, 2H), 7.60 (s, 1H), 7.50–7.41 (m, 2H), 4.06 (s, 3H), 4.05 (s, 3H); MS (APCI) *m/z* 288.0626, calcd for C₁₅H₁₃NO₃S [M + H]⁺, 288.0689.

5.1.8. 4,9-Dimethoxynaphtho[2,3-*b*]thiophene-2-carbonitrile (**16**)

A solution of oxime **15** (2.00 g, 7.0 mmol) in acetic anhydride (50 mL) was refluxed for 4 h. It was allowed to cool to rt and then poured onto ice-water (200 mL). The precipitate was filtered by suction and purified by chromatography to afford a yellow powder; 65% yield; mp 167–168 °C; FTIR 2210 (CN), 1585 cm⁻¹; ¹H NMR (CDCl₃) δ 8.21 (dd, *J* = 8.0, 1.3 Hz, 1H), 8.14 (dd, *J* = 7.5, 0.8 Hz, 1H), 8.07 (s, 1H), 7.57–7.46 (m, 2H), 4.07 (s, 3H), 4.05 (s, 3H); MS (APCI) *m/z* 270.0513, calcd for C₁₅H₁₁NO₂S [M + H]⁺, 270.0583.

5.1.9. *N'*-Hydroxy-4,9-dimethoxynaphtho[2,3-*b*]thiophene-2-carboximidamide (**17**)

Hydroxylamine hydrochloride (0.26 g, 3.71 mmol) in methanol (20 mL) was added to a solution of sodium (85 mg, 3.71 mmol) in methanol (10 mL), and the mixture was stirred for 40 min at rt. A

precipitate was filtered off, and the filtrate was treated with **16** (1.00 g, 3.71 mmol) and refluxed for 18 h. Then it was cooled and the solvent evaporated under vacuum. The residue was purified by chromatography to afford a yellow powder; 34% yield; mp 215–216 °C; FTIR 1643, 1589 cm⁻¹; ¹H NMR (CDCl₃) δ 8.19–8.11 (m, 2H), 7.65 (s, 1H), 7.49–7.42 (m, 2H), 4.06 (s, 3H), 4.05 (s, 3H); MS (APCI) *m/z* 303.0705, calcd for C₁₅H₁₄N₂O₃S [M + H]⁺, 303.0798.

5.1.10. 5-Ethyl-3-(4,9-dimethoxynaphtho[2,3-*b*]thiophen-2-yl)-1,2,4-oxadiazole (**18**)

Propionic acid (0.18 g, 2.47 mmol) in dry CH₂Cl₂ (20 mL) at 0 °C under N₂ was treated with DCC (0.26 g, 1.24 mmol) and stirred for 1 h. A precipitate was filtered off, and the solvent was evaporated. The residue was treated with pyridine (20 mL), and a solution of **17** (0.36 g, 1.19 mmol) in pyridine (4 mL) was added. Then the mixture was refluxed for 3 h, cooled to rt, poured onto ice-water (200 mL), acidified with HCl (2 mol/L), and extracted with CH₂Cl₂ (3 × 50 mL). The combined organic phase was successively washed with water (2 × 200 mL), a saturated solution of NaHCO₃ (2 × 200 mL), HCl (2 mol/L, 2 × 200 mL), and a saturated solution of NaCl (2 × 200 mL). Then it was dried over Na₂SO₄, concentrated, and the residue was purified by chromatography to provide yellow crystals; 50% yield; mp 129–131 °C; FTIR 1558, 1358 cm⁻¹; ¹H NMR (CDCl₃) δ 8.23 (s, 1H), 8.23–8.12 (m, 2H), 7.47 (m, 2H), 4.09 (s, 3H), 4.09 (s, 3H), 2.96 (q, *J* = 7.6 Hz, 2H), 1.42 (t, *J* = 7.6 Hz, 3H); MS *m/z* 341.0860, calcd for C₁₈H₁₆N₂O₃S [M + H]⁺, 341.0954.

5.1.11. 2-(5-Ethyl-1,2,4-oxadiazol-3-yl)naphtho[2,3-*b*]thiophene-4,9-dione (**19**)

This was prepared from **18** as described for **6** to afford a yellow powder; 63% yield; mp 156–158 °C; FTIR 1662, 1573 cm⁻¹; ¹H NMR (CDCl₃) δ 8.25 (s, 1H), 8.19 (m, 2H), 7.73 (m, 2H), 2.95 (q, *J* = 7.6 Hz, 2H), 1.41 (t, *J* = 7.6 Hz, 3H); ¹³C NMR (CDCl₃) δ 181.73, 178.83, 178.13, 163.44, 146.88, 143.00, 136.56, 134.23, 133.95, 133.56, 133.27, 127.84, 127.51, 127.08, 20.31, 10.71; MS *m/z* 311.0417, calcd for C₁₆H₁₀N₂O₃S [M + H]⁺, 311.0485.

An anthraquinone-based analogue **19a** and its precursors **15a–18a** were also prepared, as described above for **19** and **15–18**, respectively. See Supplementary content for details.

5.1.12. Methyl 4,9-Dimethoxynaphtho[2,3-b]thiophene-2-carboxylate (20)

To the carboxylic acid **9a** (1.50 g, 5.20 mmol) in absolute methanol (0.63 mL, 15.60 mmol) was added DMAP (0.05 g, 0.41 mmol) under stirring. Then DCC (1.18 g, 5.72 mmol) was added at 0 °C, and the mixture was stirred for 10 min, then for an additional 3 h at rt. The mixture was filtered, the filtrate evaporated and dissolved in CH₂Cl₂ (100 mL). The solution was washed with HCl (0.5 mol/L, 2 × 50 mL), then with a saturated solution of NaHCO₃ (2 × 50 mL), and the organic phase was dried over Na₂SO₄. Then the solvent was evaporated and the product purified by chromatography to give yellow crystals; 89% yield; mp 162 °C; FTIR 1710 (CO) cm⁻¹; ¹H NMR (CDCl₃) δ 8.20 (m, 2H), 8.18 (s, 1H), 7.84–7.71 (m, 2H), 4.28 (s, 3H), 4.05 (s, 3H), 4.01 (s, 3H); MS (APCI) *m/z* 303.0678, calcd for C₁₆H₁₄O₄S [M + H]⁺, 303.0686.

5.1.13. 4,9-Dimethoxynaphtho[2,3-b]thiophene-2-carbohydrazide (21)

To a solution of hydrazine hydrate (1.72 g, 1.67 mL, 34.44 mmol) in ethanol (25 mL) was added **20** (2.60 g, 8.61 mmol) in small portions. The mixture was refluxed for 5 h, and the residue was filtered and washed with hexane to afford a light yellow powder; 66% yield; mp 210 °C; FTIR 1620, 1589 cm⁻¹; ¹H NMR (DMSO-*d*₆) δ 10.21 (s, 1H), 8.33 (s, 1H), 8.26–8.19 (m, 1H), 8.16–8.11 (m, 1H), 7.65–7.54 (m, 2H), 4.11 (s, 3H), 4.05 (s, 3H); ¹³C NMR (DMSO-*d*₆) δ 160.88, 148.00, 145.25, 138.78, 130.95, 128.54, 126.40, 125.37, 125.33, 125.07, 122.33, 121.16, 120.99, 63.13, 60.68; MS (APCI) *m/z* 303.0808, calcd for C₁₅H₁₄N₂O₃S [M + H]⁺, 303.0798.

5.1.14. 2-(4,9-Dimethoxynaphtho[2,3-*b*]thiophen-2-yl)-1,3,4-oxadiazole (**22a**)

Hydrazide **21** (0.20 g, 0.66 mmol), trimethyl orthoformate (84 mg, 0.087 mL, 0.79 mmol) and the catalyst Nafion[®]NR50 (40 mg) were placed in a 10 mL microwave reaction vessel equipped with a magnetic stirrer. The mixture was heated to 130 °C and irradiated at 40–140 W for 25 min. The product was purified by chromatography to afford a yellow powder; 51% yield; mp 147–149 °C; FTIR 1597 cm⁻¹; ¹H NMR (CDCl₃) δ 8.45 (s, 1H), 8.23–8.19 (m, 2H), 8.15 (s, 1H), 7.54–7.45 (m, 2H), 4.10 (s, 3H), 4.09 (s, 3H); ¹³C NMR (CDCl₃) δ 161.05, 152.62, 148.93, 146.25, 130.81, 129.08, 126.82, 126.58, 126.07, 125.55, 124.62, 124.44, 122.67, 121.44, 63.64, 60.96; MS (APCI) *m/z* 313.0650, calcd for C₁₆H₁₂N₂O₃S [M + H]⁺, 313.0641.

In a similar fashion, compounds **22b–22e** and **23a–23c** were prepared from the appropriate orthoesters. See Supplementary content for details.

5.1.15. 5-(4,9-Dimethoxynaphtho[2,3-*b*]thiophen-2-yl)-1H-tetrazole (**26**)

To a solution of **16** (0.23 g, 0.86 mmol) in DMF (100 mL) was added NaN₃ (0.62 g, 9.50 mmol) and NH₄Cl (0.51 g, 9.50 mmol), and the mixture was stirred at 90 °C for 5 h. Then it was poured onto ice-water (200 mL), and the precipitate was filtered off. The filtrate was acidified with 36% HCl to afford an additional precipitate. Purification by chromatography provided a yellow powder; 78% yield; mp 251–252 °C; FTIR 1660, 1620 cm⁻¹; ¹H NMR (DMSO-*d*₆) δ 8.26 (s; 1H), 8.20–8.15 (m; 2H), 7.90–7.79 (m; 2H), 4.20 (s; 3H), 4.05 (s; 3H); MS *m/z* 312 (55, M⁺), 268 (100).

5.1.16. (*E*)-4-(4,9-Dimethoxynaphtho[2,3-*b*]thiophen-2-yl)but-3-en-2-one (**27**)

To a solution of **14** (0.32 g, 1.18 mmol) in acetone (30 mL) and MeOH (30 mL) under N₂ was added KOH (15 %, 0.60 mL), and the mixture was stirred for 6 h under N₂ at rt. Then it was poured

onto ice-water (30 mL) and acidified with glacial acetic acid (pH 4). The precipitate was washed with water, dried under vacuum and purified by chromatography (petroleum ether/EtOAc, 8/2) to afford bright orange crystals: 73 % yield; mp 214 °C; FTIR: 1667, 1566 cm^{-1} ; ^1H NMR (CDCl_3) δ 8.24 (dd, $J = 1.4, 7.5$ Hz, 1H), 8.18 (dd, $J = 1.5, 7.6$ Hz, 1H), 7.79–7.73 (m, 2H), 7.58–7.47 (m, 2H), 6.60 (d, $J = 15.8$ Hz, 1H), 4.13 (s, 6H), 2.40 (s, 3H); ^{13}C NMR (101 MHz, CDCl_3) δ 197.46, 148.39, 146.07, 140.35, 135.98, 131.69, 129.13, 128.64, 126.95, 126.92, 126.43, 126.15, 125.48, 122.79, 121.56, 63.52, 60.92, 28.27; MS (APCI) m/z 313.0895, calcd for $\text{C}_{18}\text{H}_{16}\text{O}_3\text{S}$ [$\text{M} + \text{H}$] $^+$, 313.0893.

In a similar fashion, compound **28** was prepared from acetophenone. See Supplementary content for details.

5.1.17. 2-((2-Methylhydrazono)methyl)naphtho[2,3-*b*]thiophene-4,9-dione (**37**)

To a solution of **32** (0.23 g, 0.95 mmol) in benzene (40 mL) was added methylhydrazine (44 mg, 50 μL , 0.95 mmol), and the mixture was stirred at rt for 12 h. The solvent was evaporated and the residue was purified by chromatography to afford a dark red powder; 21% yield; mp 289 °C; FTIR 3313, 1666, 1643, 1577 cm^{-1} ; ^1H NMR ($\text{DMSO-}d_6$) δ 8.39 (d, $J = 4.4$ Hz, 1H), 8.12–8.04 (m, 2H), 7.88–7.83 (m, 2H), 7.62 (s, 1H), 7.51 (s, 1H), 2.86 (d, $J = 3.6$ Hz, 3H); ^{13}C NMR ($\text{DMSO-}d_6$) δ 179.49, 177.50, 153.64, 143.69, 140.51, 134.53, 134.37, 133.90, 133.23, 127.16, 126.61, 123.52, 121.46, 33.43; MS (APCI) m/z 271.0566, calcd for $\text{C}_{14}\text{H}_{10}\text{N}_2\text{O}_2\text{S}$ [$\text{M} + \text{H}$] $^+$, 271.0536.

Analogously, compound **38** was prepared from phenylhydrazine. See Supplementary content for details.

5.1.18. 2-Nitronaphtho[2,3-*b*]thiophene-4,9-dione (**39a**)

This was obtained in a similar fashion as described [40], together with **39b**. For details and crystallographic data of **39a** and **39b**, see the Supplementary content.

5.1.19. 2-Aminonaphtho[2,3-*b*]thiophene-4,9-dione (**40**)

To a solution of **39a** (1.5 g, 5.8 mmol) and tetrabutylammonium bromide (16 mg, 0.05 mmol) in THF (100 mL) under N₂ at 0 °C was added dropwise with vigorous stirring a solution of sodium dithionite (3.33 g, 19.14 mmol) in water (50 mL). The solution was allowed to warm to rt and stirred for an additional 30 min. Then the solution was extracted with CH₂Cl₂ (3 × 100 mL), the solvent was evaporated and the residue was purified by chromatography (CH₂Cl₂/EtOAc, 1/1) to afford dark violet crystals; 44% yield; mp 292 °C; FTIR 3326, 1656, 1610, 1590 cm⁻¹; ¹H NMR (DMSO-*d*₆) δ 8.07–8.03 (m, 2H), 7.86–7.78 (m, 2H), 7.67 (s, 2H), 6.34 (s, 1H); MS (APCI) *m/z* 230.0270, calcd for C₁₂H₇NO₂S [M + H]⁺, 230.02703.

5.1.20. *N*-(4,9-Dioxo-4,9-dihydronaphtho[2,3-*b*]thiophen-2yl)propionamide (**41a**)

To a solution of **40** (58.1 mg, 0.26 mmol) in pyridine (5 mL) at 0 °C was added dropwise propionyl chloride (70.5 mg, 0.76 mmol). The solution was allowed to warm to rt and stirred for an additional 2 h. Then CH₂Cl₂ (20 mL) was added, and the solution was extracted with HCl (2 mol/L, 3 × 20 mL). The combined aqueous phase was extracted with CH₂Cl₂ (3 × 20 mL), and the combined organic phase was dried over Na₂SO₄. Then it was concentrated and the residue was purified by chromatography (CH₂Cl₂/EtOAc, 9/1) to afford orange-brown crystals; 56% yield; mp 294–296 °C; FTIR 3325, 1670, 1632, 1589 cm⁻¹; ¹H NMR (DMSO-*d*₆) δ 8.09–8.06 (m, 2H), 7.87–7.82 (m, 2H), 7.06 (s, 1H), 2.47 (q, *J* = 7.5 Hz, 2H), 1.11 (t, *J* = 7.5 Hz, 3H); MS (APCI) *m/z* 286.0532, calcd for C₁₅H₁₁NO₃S [M + H]⁺, 286.05324.

In a similar fashion, compounds **41b–41e** were prepared from the appropriate acyl chlorides. See Supplementary content for details.

Compounds **7** [30], **42** [64], and **43** [30] were prepared as described.

5.2. *Biological assay methods*

5.2.1. *Keratinocyte culture and determination of cell hyperproliferation*

HaCaT keratinocytes [42] were obtained from CLS cell lines service (Eppelheim, Germany). The cell line was confirmed as mycoplasma negative using MycoAlert™ (Lonza, Basel) mycoplasma detection kit, and then the assay was performed as described previously [65]. After 48 h of incubation with the test compounds in a 96-well microtiter plate, MTT [3-(4,5-dimethylthiazol-2-yl)-2,5-diphenyltetrazolium bromide] (20 μ L of a 5 mg/mL solution in PBS) was added to each well and the plate was incubated for 2 h at 37 °C. Then the plate was centrifuged (1500g for 10 min) and unreduced MTT removed. DMSO (100 μ L) was added to dissolve the blue formazan. The absorbance at 570 nm (with background subtraction at 630 nm) was read using a Spectra Max 384 Plus microplate reader (Molecular Devices). Appropriate blanks were performed with MTT. Cell numbers were calculated from blank-subtracted absorbance, and data were analyzed with the software Softmax Pro. Inhibition was calculated by the comparison of the mean values of the test compound ($N = 3$, $SD < 10\%$) with the control ($N = 6–8$) activity: $(1 - \text{test compound/control}) \times 100$. Inhibition was statistically significant compared to that of the control (Student's t-test; $P < 0.05$). IC_{50} values were obtained by nonlinear regression (GraphPad Prism).

5.2.2. Superoxide generation assays (enzymatic one-electron reduction, enzymatic two-electron reduction)

The rate of superoxide generation was measured using succinoylated cytochrome *c* as the terminal electron acceptor. The superoxide-dependent extent of cytochrome *c* reduction was confirmed by addition of superoxide dismutase (SOD), and the generation of H₂O₂ and hydroxyl radicals were prevented with catalase and DTPA. Both assays were performed exactly as previously described in full detail [28].

5.2.3. Intracellular superoxide generation

In order to detect intracellular superoxide levels [66], HaCaT keratinocytes were cultivated as described [65]. Cells were grown in Dulbecco's modified Eagle's medium (DMEM, No. E15-810, PAA) in 6-well plates (2.5×10^5 cells/mL) supplemented with 10% fetal bovine serum, penicillin (100 units/mL), and streptomycin (100 µg/mL) in a CO₂ incubator for 24 h at 37 °C. Then the medium was replaced, and cells were treated for 18 h (chronic treatment) with the test compound (5 µM, DMSO, final concentration of DMSO in the culture medium was 0.1%) in CO₂ incubator for 24 h at 37 °C. Also, acute treatment experiments (30 min, 50 µM test compound) were carried out. In a separate set of experiments, keratinocytes were preincubated with the NQO-1 inhibitor dicoumarol [50,58] (5 µmol/L) for 25 min before treatment the test compounds were added. After incubation with the test compound, DHE (10 µmol/mL) was added, the cell culture plates were treated on a shaker (200 rpm) for 5 min, and the cells were allowed to load DHE for an additional 25 min under incubation conditions. Then the medium was removed, the cells were washed with PBS (0.5 mL/well), trypsinized (0.3 mL/well) for 7 min, treated with FACS buffer (FACSFlow, BD Biosciences, no. 342003, 0.7 mL), centrifuged ($1000 \times g$), and resuspended in FACS buffer (0.5 mL). Experiments with DHE were performed in the dark. Controls were performed with no DHE

and with no test compound (DMSO alone). DHE-treated keratinocytes were immediately evaluated by flow cytometric measurements, which were performed at different time points (0, 10, 20, 30, 60, and 90 min). Keratinocytes were kept in CO₂ incubator at 37 °C between measurements. All experiments were run in triplicate.

5.2.4. Flow cytometry

The fluorescence of the oxidized product 2-OH-E⁺ was monitored on a FACSCalibur (Becton Dickinson) flow cytometer equipped with an argon laser ($\lambda = 488$ nm) as a light source, and the data were collected in the FL2 channel ($\lambda = 550$ -600 nm, 42 nm bandpass). For each sample, 10 000 live cells were examined, and dead cells were gated out for analysis. The recorded histograms were analyzed using the software CellQuest Pro and were compared with the histograms of untreated control cells. Data are expressed as mean fluorescence intensity (MFI).

5.2.5. Flow cytometric detection of 7-aminoactinomycin D (7-AAD) positive cells

Cells were grown and exposed to test compounds or preincubated with dicoumarol exactly as described above. Evaluation of apoptosis [61] was performed using 7-AAD (10 μ g/mL) according to the manufacturer's instructions. At least 10 000 cells were acquired, and data were collected in the FL3 channel and analyzed by CellQuest Pro.

Appendix A. Supplementary data

Chemical data of compounds **9b**, **9c**, **13b–13u**, **15a–19a**, **22b–22e**, **23a–23c**, **24a–24e**, **25a–25c**, **28–36**, **38**, **39a**, **39b**, **41b–41e**, X-ray structures of **39a**, **39b**, purity of tested compounds, NMR

spectra, and certificate of analysis of the human keratinocyte cell line can be found at: see Supplementary content.

Captions of Figures, Schemes and Charts

Figure 1. Redox cycling of naphtho[2,3-*b*]thiophene-4,9-diones initiated through one-electron reduction by CPR/NADPH to the semiquinone radical and two-electron reduction by NQO-1/NADPH to the hydroquinone.

Figure 2. Lapacho quinones (**1–3**), synthetic analogues (**5, 6**) and anthralin (**4**)

Scheme 1. Reagents: (a) $\text{Na}_2\text{S}_2\text{O}_4$, Bu_4NBr , THF, KOH, Me_2SO_4 , N_2 ; (b) K_2CO_3 , methyl tosylate, MeCN; (c) *n*-BuLi, THF, $-30\text{ }^\circ\text{C}$, dry ice, N_2 ; (d) DCC, CH_2Cl_2 , $0\text{ }^\circ\text{C}$, *N*-hydroxypropionamidine, pyridine, reflux; (e) $(\text{NH}_4)_2[\text{Ce}(\text{NO}_3)_6]$, MeCN, H_2O , $0\text{ }^\circ\text{C}$; (f) BBr_3 , CH_2Cl_2 , $0\text{ }^\circ\text{C}$.

Scheme 2. Reagents: (a) DCC, CH₂Cl₂, 0 °C, *N*-hydroxypropionamidine, pyridine, reflux (R is defined in Charts 1–4); (b) (NH₄)₂[Ce(NO₃)₆], MeCN, H₂O, 0 °C; (f) BBr₃, CH₂Cl₂, 0 °C (see Chart 2).

Scheme 3. Reagents: (a) NH₂OH • HCl, Na₂CO₃, MeOH, reflux; (b) Ac₂O, reflux; (c) NH₂OH • HCl, Na, MeOH, reflux; (d) propionic acid, DCC, CH₂Cl₂, 0 °C, N₂, pyridine, reflux; (e) (NH₄)₂[Ce(NO₃)₆], MeCN, H₂O, 0 °C.

Scheme 4. Reagents: (a) DCC, DMAP, 0 °C, rt; (b) N₂H₄, EtOH, reflux; (c) appropriate orthoester, Nafion[®]NR50, microwave 40–140 W, 130 °C; (d) appropriate orthoester, P₄S₁₀/Al₂O₃, MeCN (dioxane), reflux, N₂; (e) (NH₄)₂[Ce(NO₃)₆], MeCN, H₂O, 0 °C.

Scheme 5. Reagents: (a) *n*-BuLi, THF, -30 °C, appropriate *N,N*-dimethylcarboxamide, rt, N₂; (b) NaN₃, NH₄Cl, DMF, 90 °C; (c) KOH, EtOH, acetone or acetophenone, rt (0 °C); (d) (NH₄)₂[Ce(NO₃)₆], MeCN, H₂O, 0 °C; (e) appropriate hydrazine, benzene, rt.

Scheme 6. Reagents: (a) conc. HNO₃, conc. H₂SO₄ 0 °C; reflux; (b) Na₂S₂O₄, Bu₄NBr, rt; (c) appropriate acyl chloride, pyridine, rt.

Chart 1. Suppression of human keratinocyte hyperproliferation by non-quinoid analogues; IC₅₀ values (μmol/L) against HaCaT keratinocyte growth in parentheses.

Chart 2. Suppression of human keratinocyte hyperproliferation by quinoid analogues; IC₅₀ values (μmol/L) against HaCaT keratinocyte growth in parentheses.

Chart 3. Suppression of human keratinocyte hyperproliferation by quinoid analogues; IC₅₀ values (μmol/L) against HaCaT keratinocyte growth in parentheses.

Chart 4. Suppression of human keratinocyte hyperproliferation by quinoid analogues; IC₅₀ values (μmol/L) against HaCaT keratinocyte growth in parentheses.

References

- [1] K.W. Wellington, Understanding cancer and the anticancer activities of naphthoquinones - a review, *RSC Advances* 5 (2015) 20309-20338.
- [2] L. Costantino, D. Barlocco, Privileged structures as leads in medicinal chemistry, *Curr. Med. Chem.* 13 (2006) 65-85.
- [3] S.L. de Castro, F.S. Emery, E.N. da Silva Jr., Synthesis of quinoidal molecules: strategies towards bioactive compounds with an emphasis on lapachones, *Eur. J. Med. Chem.* 69 (2013) 678-700.
- [4] V.K. Tandon, S. Kumar, Recent development on naphthoquinone derivatives and their therapeutic applications as anticancer agents, *Expert Opin. Ther. Pat.* 23 (2013) 1087-1108.
- [5] Y. Song, G.R. Buettner, Thermodynamic and kinetic considerations for the reaction of semiquinone radicals to form superoxide and hydrogen peroxide, *Free Radical Biol. Med.* 49 (2010) 919-962.

- [6] M. Doering, L.A. Ba, N. Lilienthal, C. Nicco, C. Scherer, M. Abbas, A.A.P. Zada, R. Coriat, T. Burkholz, L. Wessjohann, M. Diederich, F. Batteux, M. Herling, C. Jacob, Synthesis and selective anticancer activity of organochalcogen based redox catalysts, *J. Med. Chem.* 53 (2010) 6954-6963.
- [7] E.N. da Silva Jr., B.C. Cavalcanti, T.T. Guimaraes, M.d.F.R. Pinto, I.O. Cabral, C. Pessoa, L.V. Costa-Lotuf, M.O. de Moraes, C.K.Z. de Andrade, M.R. dos Santos, C.A. de Simone, M.O.F. Goulart, A.V. Pinto, Synthesis and evaluation of quinonoid compounds against tumor cell lines, *Eur. J. Med. Chem.* 46 (2011) 399-410.
- [8] F. Lizzi, G. Veronesi, F. Belluti, C. Bergamini, A. López-Sánchez, M. Kaiser, R. Brun, R.L. Krauth-Siegel, D.G. Hall, L. Rivas, M.L. Bolognesi, Conjugation of quinones with natural polyamines: toward an expanded antitrypanosomatid profile, *J. Med. Chem.* 55 (2012) 10490-10500.
- [9] J.Z. Li, Y. Ke, H.P. Misra, M.A. Trush, Y.R. Li, H. Zhu, Z. Jia, Mechanistic studies of cancer cell mitochondria- and NQO1-mediated redox activation of beta-lapachone, a potentially novel anticancer agent, *Toxicol. Appl. Pharmacol.* 281 (2014) 285-293.
- [10] F. Prati, C. Bergamini, M.T. Molina, F. Falchi, A. Cavalli, M. Kaiser, R. Brun, R. Fato, M.L. Bolognesi, 2-Phenoxy-1,4-naphthoquinones: from a multitarget antitrypanosomal to a potential antitumor profile, *J. Med. Chem.* 58 (2015) 6422-6434.
- [11] A.A. Vieira, I.R. Brandao, W.O. Valenca, C.A. de Simone, B.C. Cavalcanti, C. Pessoa, T.R. Carneiro, A.L. Braga, E.N. da Silva, Hybrid compounds with two redox centres: Modular synthesis of chalcogen-containing lapachones and studies on their antitumor activity, *Eur. J. Med. Chem.* 101 (2015) 254-265.
- [12] A.R. Burnett, R.H. Thomson, Naturally occurring quinones. Part X. The quinoid constituents of *Tabebuia avellaneda* (Bignoniaceae), *J. Chem. Soc. C* (1967) 2100-2104.

- [13] M.M. Rao, D.G.I. Kingston, Plant anticancer agents. XII. Isolation and structure elucidation of new cytotoxic quinones from *Tabebuia cassinoides*, *J. Nat. Prod.* 45 (1982) 600-604.
- [14] F. Epifano, S. Genovese, S. Fiorito, V. Mathieu, R. Kiss, Lapachol and its congeners as anticancer agents: a review, *Phytochem. Rev.* 13 (2014) 37-49.
- [15] K. Jones, *Pau d'arco: immune Power from the Rain Forest*, Healing Arts Press, Rochester, VT, 1995.
- [16] J.R. Gómez Castellanos, J.M. Prieto, M. Heinrich, Red lapacho (*Tabebuia impetiginosa*)--a global ethnopharmacological commodity?, *J. Ethnopharmacol.* 121 (2009) 1-13.
- [17] A. Takano, K. Hashimoto, M. Ogawa, J. Koyanagi, T. Kurihara, H. Wakabayashi, H. Kikuchi, Y. Nakamura, N. Motohashi, H. Sakagami, K. Yamamoto, A. Tanaka, Tumor-specific cytotoxicity and type of cell death induced by naphtho[2,3-*b*]furan-4,9-diones and related compounds in human tumor cell lines: relationship to electronic structure, *Anticancer Res.* 29 (2009) 455-464.
- [18] M. Yamashita, M. Kaneko, H. Tokuda, K. Nishimura, Y. Kumeda, A. Iida, Synthesis and evaluation of bioactive naphthoquinones from the Brazilian medicinal plant, *Tabebuia avellanedae*, *Bioorg. Med. Chem.* 17 (2009) 6286-6291.
- [19] S. Jiménez-Alonso, J. Guasch, A. Estévez-Braun, I. Ratera, J. Veciana, A.G. Ravelo, Electronic and cytotoxic properties of 2-amino-naphtho[2,3-*b*]furan-4,9-diones, *J. Org. Chem.* 76 (2011) 1634-1643.
- [20] I. Gomez-Monterrey, P. Campiglia, C. Aquino, A. Bertamino, I. Granata, A. Carotenuto, D. Brancaccio, P. Stiuso, I. Scognamiglio, M.R. Rusciano, A.S. Maione, M. Illario, P. Grieco, B. Maresca, E. Novellino, Design, synthesis, and cytotoxic evaluation of acyl derivatives of 3-aminonaphtho[2,3-*b*]thiophene-4,9-dione, a quinone-based system, *J. Med. Chem.* 54 (2011) 4077-4091.

- [21] P.R. Duchowicz, D.O. Bennardi, D.E. Bacelo, E.L. Bonifazi, C. Rios-Luci, J.M. Padrón, G. Burton, R.I. Misico, QSAR on antiproliferative naphthoquinones based on a conformation-independent approach, *Eur. J. Med. Chem.* 77 (2014) 176-184.
- [22] S.M. Lim, Y. Jeong, S. Lee, H. Im, H.S. Tae, B.G. Kim, H.D. Park, J. Park, S. Hong, Identification of β -lapachone analogs as novel MALT1 inhibitors to treat an aggressive subtype of diffuse large B-cell lymphoma, *J. Med. Chem.* 58 (2015) 8491-8502.
- [23] K. Müller, A. Sellmer, W. Wiegrebe, Potential antipsoriatic agents: lapacho compounds as potent inhibitors of HaCaT cell growth, *J. Nat. Prod.* 62 (1999) 1134-1136.
- [24] K. Müller, H. Reindl, K. Breu, Antipsoriatic anthrones with modulated redox properties. 5. Potent inhibition of human keratinocyte growth, induction of keratinocyte differentiation, and reduced membrane damage by novel 10-arylacetyl-1,8-dihydroxy-9(10*H*)-anthracenones, *J. Med. Chem.* 44 (2001) 814-821.
- [25] A. Zuse, P. Schmidt, S. Baasner, K.J. Böhm, K. Müller, M. Gerlach, E.G. Günther, E. Unger, H. Prinz, Sulfonate derivatives of naphtho[2,3-*b*]thiophen-4(9*H*)-one and 9(10*H*)-anthracenone as highly active antimicrotubule agents. Synthesis, antiproliferative activity, and inhibition of tubulin polymerization, *J. Med. Chem.* 50 (2007) 6059-6066.
- [26] A. Putic, L. Stecher, H. Prinz, K. Müller, Structure–activity relationship studies of acridones as potential antipsoriatic agents. 1. Synthesis and antiproliferative activity of simple *N*-unsubstituted 10*H*-acridin-9-ones against human keratinocyte growth, *Eur. J. Med. Chem.* 45 (2010) 3299-3310.
- [27] H. Prinz, B. Chamasmani, K. Vogel, K.J. Böhm, B. Aicher, M. Gerlach, E.G. Günther, P. Amon, I. Ivanov, K. Müller, *N*-Benzoylated phenoxazines and phenothiazines: synthesis, antiproliferative activity and inhibition of tubulin polymerization, *J. Med. Chem.* (2011) 4247-4263.

- [28] A. Reichstein, S. Vortherms, S. Bannwitz, J. Tentrop, H. Prinz, K. Müller, Synthesis and structure–activity relationships of lapacho analogues. 1. Suppression of human keratinocyte hyperproliferation by 2-substituted naphtho[2,3-*b*]furan-4,9-diones, activation by enzymatic one- and two-electron reduction, and intracellular generation of superoxide, *J. Med. Chem.* 55 (2012) 7273-7284.
- [29] M.A. Lowes, A.M. Bowcock, J.G. Krueger, Pathogenesis and therapy of psoriasis, *Nature* 445 (2007) 866-873.
- [30] S. Bannwitz, D. Krane, S. Vortherms, T. Kalin, C. Lindenschmidt, N. Zahedi Golpayegani, J. Tentrop, H. Prinz, K. Müller, Synthesis and structure–activity relationships of lapacho analogues. 2. Modification of the basic naphtho[2,3-*b*]furan-4,9-dione, redox activation, and suppression of human keratinocyte hyperproliferation by 8-hydroxynaphtho[2,3-*b*]thiophene-4,9-diones, *J. Med. Chem.* 57 (2014) 6226-6239.
- [31] S. Rapolu, M. Alla, V.R. Bommena, R. Murthy, N. Jain, V.R. Bommareddy, M.R. Bommineni, Synthesis and biological screening of 5-(alkyl(1H-indol-3-yl))-2-(substituted)-1,3,4-oxadiazoles as antiproliferative and anti-inflammatory agents, *Eur. J. Med. Chem.* 66 (2013) 91-100.
- [32] S. Valente, D. Trisciuglio, T. De Luca, A. Nebbioso, D. Labella, A. Lenoci, C. Bigogno, G. Dondio, M. Miceli, G. Brosch, D. Del Bufalo, L. Altucci, A. Mai, 1,3,4-Oxadiazole-containing histone deacetylase inhibitors: anticancer activities in cancer cells, *J. Med. Chem.* 57 (2014) 6259-6265.
- [33] M.M.G. El-Din, M.I. El-Gamal, M.S. Abdel-Maksoud, K.H. Yoo, C.-H. Oh, Synthesis and in vitro antiproliferative activity of new 1,3,4-oxadiazole derivatives possessing sulfonamide moiety, *Eur. J. Med. Chem.* 90 (2015) 45-52.
- [34] Q. Guan, D.J. Feng, Z.S. Bai, Y.H. Cui, D.Y. Zuo, M.A. Zhai, X.W. Jiang, W.B. Zhou, K. Bao, Y.L. Wu, W.G. Zhang, Microwave-assisted synthesis, molecular docking and

antiproliferative activity of (3/5-aryl-1,2,4-oxadiazole-5/3-yl)(3,4,5-trimethoxyphenyl)methanone oxime derivatives, *Medchemcomm* 6 (2015) 1484-1493.

- [35] V. Nieddu, G. Pinna, I. Marchesi, L. Sanna, B. Asproni, G.A. Pinna, L. Bagella, G. Murineddu, Synthesis and antineoplastic evaluation of novel unsymmetrical 1,3,4-oxadiazoles, *J. Med. Chem.* 59 (2016) 10451-10469.
- [36] S. Borg, G. Estenne-Bouhtou, K. Luthman, I. Csöreg, W. Hesselink, U. Hacksell, Synthesis of 1,2,4-oxadiazole-, 1,3,4-oxadiazole-, and 1,2,4-triazole-derived dipeptidomimetics, *J. Org. Chem.* 60 (1995) 3112-3120.
- [37] B. Neises, W. Steglich, 4-Dialkylaminopyridines as acylation catalysts. 5. Simple method for esterification of carboxylic acids, *Angew. Chem.-Int. Ed. Engl.* 17 (1978) 522-524.
- [38] V. Polshettiwar, R.S. Varma, Greener and rapid access to bio-active heterocycles: one-pot solvent-free synthesis of 1,3,4-oxadiazoles and 1,3,4-thiadiazoles, *Tetrahedron Lett.* 49 (2008) 879-883.
- [39] J. Koyanagi, K. Yamamoto, K. Nakayama, A. Tanaka, A new synthetic route to 2-substituted naphtho[2,3-*b*]furan-4,9-dione, *J. Heterocycl. Chem.* 34 (1997) 407-412.
- [40] C.L. Zani, E. Chiari, A.U. Krettli, S.M. Murta, M.L. Cunningham, A.H. Fairlamb, A.J. Romanha, Anti-plasmodial and anti-trypanosomal activity of synthetic naphtho[2,3-*b*]thiophen-4,9-quinones, *Bioorg. Med. Chem.* 5 (1997) 2185-2192.
- [41] N.O.V. Sonntag, The reactions of aliphatic acid chlorides, *Chem. Rev.* 52 (1953) 237-416.
- [42] P. Boukamp, R.T. Petrussevska, D. Breitkreutz, J. Hornung, A. Markham, N.E. Fusenig, Normal keratinization in a spontaneously immortalized aneuploid human keratinocyte cell line, *J. Cell Biol.* 106 (1988) 761-771.
- [43] S.E. George, R.J. Anderson, A. Cunningham, M. Donaldson, P.W. Groundwater, Evaluation of a range of anti-proliferative assays for the preclinical screening of anti-psoriatic drugs: a

comparison of colorimetric and fluorimetric assays with the thymidine incorporation assay, *Assay Drug Dev Technol* 8 (2010) 384-395.

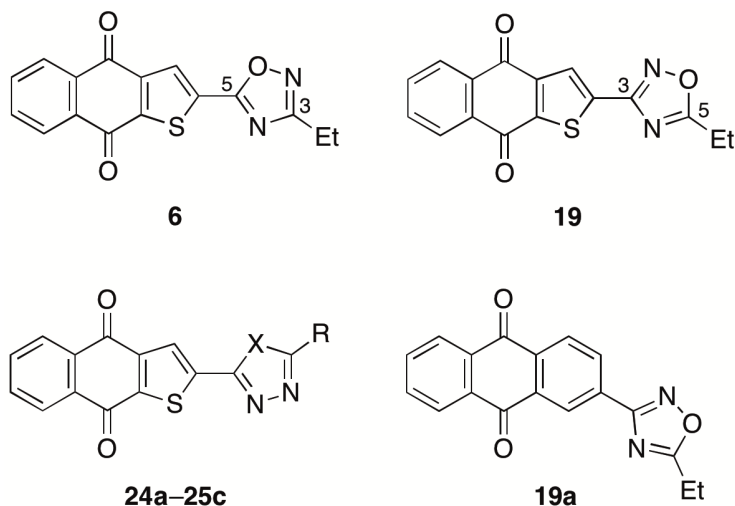
- [44] A. Brunmark, E. Cadenas, Redox and addition chemistry of quinoid compounds and its biological implications, *Free Radical Biol. Med.* 7 (1989) 435-447.
- [45] C. Lindenschmidt, D. Krane, S. Vortherms, L. Hilbig, H. Prinz, K. Müller, 8-Halo-substituted naphtho[2,3-b]thiophene-4,9-diones as redox-active inhibitors of keratinocyte hyperproliferation with reduced membrane-damaging properties, *Eur. J. Med. Chem.* 110 (2016) 280-290.
- [46] J. Boström, A. Hogner, A. Llinàs, E. Wellner, A.T. Plowright, Oxadiazoles in medicinal chemistry, *J. Med. Chem.* 55 (2012) 1817-1830.
- [47] G.A. Patani, E.J. LaVoie, Bioisosterism: A rational approach in drug design, *Chem. Rev.* 96 (1996) 3147-3176.
- [48] H. Sies, Biochemistry of oxidative stress, *Angew. Chem. Int. Ed. Engl.* 25 (1986) 1058-1071.
- [49] B. Halliwell, Oxidative stress and cancer: have we moved forward?, *Biochem J* 401 (2007) 1-11.
- [50] H. Thor, M.T. Smith, P. Hartzell, G. Bellomo, S.A. Jewell, S. Orrenius, The metabolism of menadione (2-methyl-1,4-naphthoquinone) by isolated hepatocytes. A study of the implications of oxidative stress in intact cells, *J Biol Chem* 257 (1982) 12419-12425.
- [51] G.D. Buffinton, K. Öllinger, A. Brunmark, E. Cadenas, DT-diaphorase-catalysed reduction of 1,4-naphthoquinone derivatives and glutathionyl-quinone conjugates. Effect of substituents on autoxidation rates, *Biochem J* 257 (1989) 561-571.
- [52] R.A. Kemper, M.A. Taub, M.S. Bogdanffy, Metabolism: a determinant of toxicity, in: A.W. Hayes, C.L. Kruger (Eds.) *Hayes' Principles and Methods of Toxicology*, Sixth Edition, CRC Press, Boca Raton, 2014, pp. 141-214.

- [53] E.H.G. da Cruz, M.A. Silvers, G.A.M. Jardim, J.M. Resende, B.C. Cavalcanti, I.S. Bomfim, C. Pessoa, C.A. de Simone, G.V. Botteselle, A.L. Braga, D.K. Nair, I.N.N. Namboothiri, D.A. Boothman, E.N. da Silva Júnior, Synthesis and antitumor activity of selenium-containing quinone-based triazoles possessing two redox centres, and their mechanistic insights, *Eur. J. Med. Chem.* 122 (2016) 1-16.
- [54] H. Zhao, S. Kalivendi, J. Joseph, H. Zhang, J. Joseph, K. Nithipatikom, J. Vásquez-Vivar, B. Kalyanaraman, Superoxide reacts with hydroethidine but forms a fluorescent product that is distinctly different from ethidium: potential implications in intracellular fluorescence detection of superoxide, *Free Radical Biol. Med.* 34 (2003) 1359-1368.
- [55] H. Zhao, J. Joseph, H.M. Fales, E.A. Sokoloski, R.L. Levine, J. Vasquez-Vivar, B. Kalyanaraman, Detection and characterization of the product of hydroethidine and intracellular superoxide by HPLC and limitations of fluorescence, *Proc. Natl. Acad. Sci. U.S.A.* 102 (2005) 5727-5732.
- [56] J. Zielonka, J. Vasquez-Vivar, B. Kalyanaraman, Detection of 2-hydroxyethidium in cellular systems: a unique marker product of superoxide and hydroethidine, *Nat Protoc* 3 (2008) 8-21.
- [57] G.N. De Iuliis, J.K. Wingate, A.J. Koppers, E.A. McLaughlin, R.J. Aitken, Definitive evidence for the nonmitochondrial production of superoxide anion by human spermatozoa, *J Clin Endocrinol Metab* 91 (2006) 1968-1975.
- [58] A.S. Tan, M.V. Berridge, Evidence for NAD(P)H:quinone oxidoreductase 1 (NQO1)-mediated quinone-dependent redox cycling via plasma membrane electron transport: a sensitive cellular assay for NQO1, *Free Radical Biol. Med.* 48 (2010) 421-429.
- [59] J.H. Tocher, Reductive activation of nitroheterocyclic compounds, *Gen Pharmacol* 28 (1997) 485-487.

- [60] H. Kappus, Overview of enzyme systems involved in bioreduction of drugs and in redox cycling, *Biochem. Pharmacol.* 35 (1986) 1-6.
- [61] N.C.L. Zembruski, V. Stache, W.E. Haefeli, J. Weiss, 7-Aminoactinomycin D for apoptosis staining in flow cytometry, *Anal. Biochem.* 429 (2012) 79-81.
- [62] M.L. Tedjamulia, Y. Tominaga, R.N. Castle, M.L. Lee, The synthesis of dinaphthothiophenes, *J. Heterocycl. Chem.* 20 (1983) 1143-1148.
- [63] A. Zuse, P. Schmidt, S. Baasner, K.J. Böhm, K. Müller, M. Gerlach, E.G. Günther, E. Unger, H. Prinz, 9-Benzylidene-naphtho[2,3-*b*]thiophen-4-ones as novel antimicrotubule agents – Synthesis, antiproliferative activity, and inhibition of tubulin polymerization, *J. Med. Chem.* 49 (2006) 7816-7825.
- [64] R. Goncalves, E.V. Brown, Preparation of thiophanthrenequinone and Its derivatives. I, *J. Org. Chem.* 17 (1952) 698-704.
- [65] K. Müller, P. Leukel, K. Ziereis, I. Gawlik, Antipsoriatic anthrones with modulated redox properties. 2. Novel derivatives of chrysarobin and isochrysarobin — antiproliferative activity and 5-lipoxygenase inhibition, *J. Med. Chem.* 37 (1994) 1660-1669.
- [66] P. Mukhopadhyay, M. Rajesh, K. Yoshihiro, G. Haskó, P. Pacher, Simple quantitative detection of mitochondrial superoxide production in live cells, *Biochem Biophys Res Commun* 358 (2007) 203-208.

Table 1

Suppression of human keratinocyte hyperproliferation by various oxadiazole- and thiadiazole-substituted naphtho[2,3-*b*]thiophene-4,9-diones.



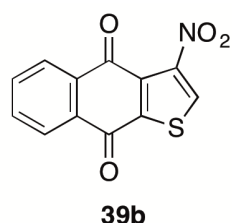
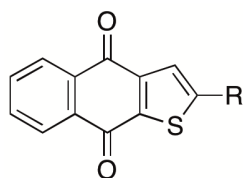
compd	R	X	AA ^a IC ₅₀ (μmol/L)
6			0.36
19			0.58
19a			> 30
24a	H	O	0.22
24b	Me	O	0.08
24c	Et	O	0.15
24d	Bu	O	1.90
24e	Ph	O	> 30
25a	H	S	0.30
25b	Me	S	3.70
25c	Et	S	> 15
anthralin			0.70
β-lapachone			0.90
menadione			15.8

^aAntihyperproliferative activity against keratinocytes. IC₅₀ = concentration of test compound required for 50% inhibition of cell growth (HaCaT). Inhibition of cell growth was significantly different with respect to that of the control, $N = 3$, $P < 0.05$.

ACCEPTED MANUSCRIPT

Table 2

Suppression of human keratinocyte hyperproliferation by naphtho[2,3-*b*]thiophene-4,9-diones bearing an open-chain substituent.



compd	R	AA ^a
		IC ₅₀ (μmol/L)
29	CO ₂ H	> 30
30	CO ₂ Me	0.71
31	CONH-NH ₂	1.7
32	CHO	1.2
33	CN	0.46
34	5-(1 <i>H</i> -tetrazole)	> 30
35	CH=CH-CO-Me	> 30
36	CH=CH-CO-Ph	> 30
37	CH=N-NH-Me	> 30
38	CH=N-NH-Ph	> 30
39a	NO ₂	1.80
39b		1.10
40	NH ₂	> 30
41a	NH-CO-Et	9.6
41b	NH-CO-Pr	5.7
41c	NH-CO- <i>i</i> Pr	3.3
41d	NH-CO-Ph	2.3
41e	NH-CO-Ph-4-MeOt	1.1
42	COMe	0.44

43

Me

5.2

^aAntihyperproliferative activity against keratinocytes. IC₅₀ = concentration of test compound required for 50% inhibition of cell growth (HaCaT). Inhibition of cell growth was significantly different with respect to that of the control, $N = 3$, $P < 0.05$.

Table 3

Rates of superoxide generation by naphtho[2,3-*b*]thiophene-4,9-diones through one-electron reduction by human recombinant CPR and two-electron reduction by human recombinant NQO-1.

cmpd	R	O ₂ ^{•-} (CPR) ^a	O ₂ ^{•-} (NQO-1) ^b
6	1,2,4-oxadiazole	0.9 ± 0.1 ^c	0.5 ± 0.1 ^c
7	H	1.2 ± 0.1 ^c	0.2 ± 0.1
39a	NO ₂	2.0 ± 0.3 ^c	4.6 ± 2.1 ^c
40	NH ₂	1.1 ± 0.4 ^c	0.8 ± 0.2 ^c
42	COMe	1.2 ± 0.1 ^c	0.8 ± 0.1 ^c
43	Me	1.1 ± 0.2 ^c	0.3 ± 0.2 ^c
menadione		2.1 ± 0.4 ^c	1.0 ± 0.4 ^c
control ^d		0.2 ± 0.1	0.2 ± 0.1

^aSuperoxide generation in the presence of CPR is expressed as SOD-inhibitable reduction of succinoylated cytochrome c (μmol/L/min/2 mU enzyme) by the test compound (100 μmol/mL)

^bSuperoxide generation in the presence of NQO-1 is expressed as SOD-inhibitable reduction of cytochrome c (μmol/L/min/unit enzyme) by the test compound (25 μmol/mL). Each value represents the mean ± SD, *N* ≥ 3.

^cValues are significantly different from vehicle control, *P* < 0.0001. ^dRate of reduction with no test compound present (DMSO).

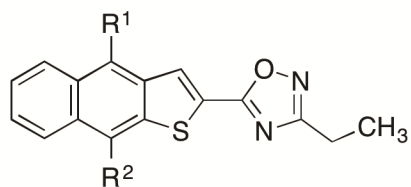
Table 4

Suppression of human keratinocyte hyperproliferation by various oxadiazole- and thiadiazole-substituted naphtho[2,3-*b*]thiophene-4,9-diones.

cmpd	acute treatment ^a O ₂ ^{•-} (MFI) ^d	chronic treatment ^b O ₂ ^{•-} (MFI) ^d	dicoumarol pretreatment ^{b, c} O ₂ ^{•-} (MFI) ^d	chronic treatment ^b apoptotic cells (%)	dicoumarol pretreatment ^{b, c} apoptotic cells (%)
6	25.2 ± 1.3 ^e	930.1 ± 153.0 ^e	558.7 ± 155.1 ^e	39.3 ± 15.8 ^e	6.9 ± 5.9
7	10.5 ± 0.1	552.7 ± 189.4 ^e	583.3 ± 33.6 ^e	4.0 ± 3.1	7.4 ± 5.4
39a	138.0 ± 40.4 ^e	973.8 ± 386.0 ^e	1022 ± 291.6 ^e	5.6 ± 1.1	3.4 ± 0.3
40	76.7 ± 8.4 ^e	518.0 ± 151.8 ^e	502.3 ± 29.4 ^e	5.6 ± 1.0	3.2 ± 0.6
42	19.2 ± 6.8 ^e	500.0 ± 230.4 ^e	434.5 ± 111.0 ^e	4.2 ± 2.4	3.7 ± 0.7
43	11.5 ± 2.1 ^e	517.0 ± 163.6 ^e	633.5 ± 33.5 ^e	4.3 ± 1.2	4.3 ± 1.1
menadione	44.0 ± 11.6 ^e	431.9 ± 83.5	457.2 ± 103.4	4.8 ± 2.3	3.1 ± 1.1
control ^f	7.1 ± 5.2	367.5 ± 80.1	407.59 ± 68.7	3.0 ± 1.0	4.3 ± 2.6

^aHaCaT keratinocytes were incubated with test compound (50 μmol/L) for 30 min. ^bHaCaT keratinocytes were incubated with test compound (5 μmol/L) for 18 h. ^cHaCaT keratinocytes were

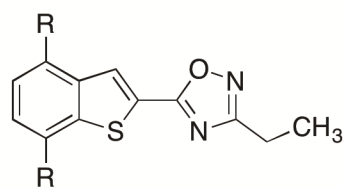
Chart 1



13a: $R^1 = R^2 = OCH_3$ (6.7 $\mu\text{mol/L}$)

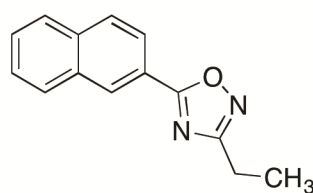
13b: $R^1 = OCH_3, R^2 = H$ ($> 30 \mu\text{mol/L}$)

13c: $R^1 = R^2 = H$ ($> 30 \mu\text{mol/L}$)



13d: $R = OCH_3$ ($> 30 \mu\text{mol/L}$)

13e: $R = H$ ($> 30 \mu\text{mol/L}$)



13f ($> 30 \mu\text{mol/L}$)

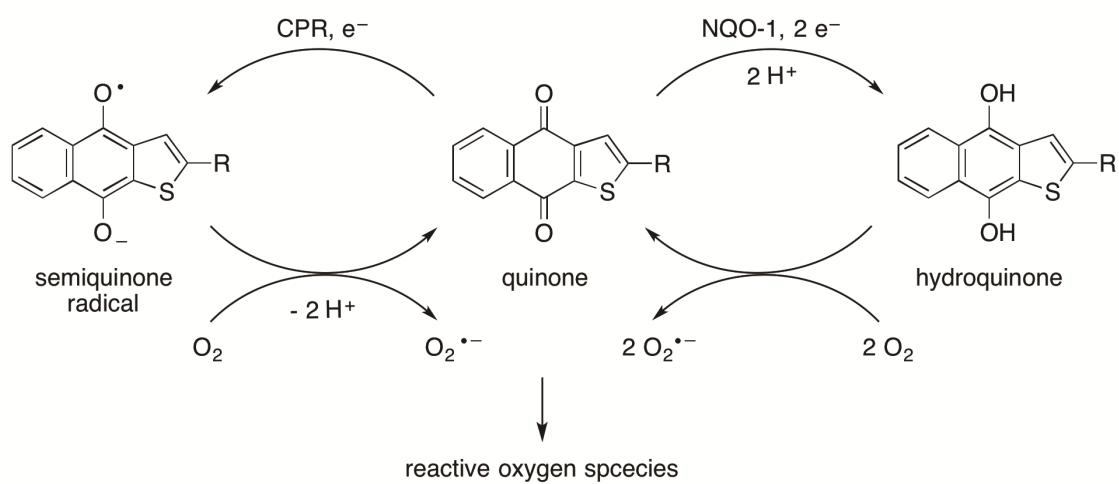


Figure 1

Scheme 1

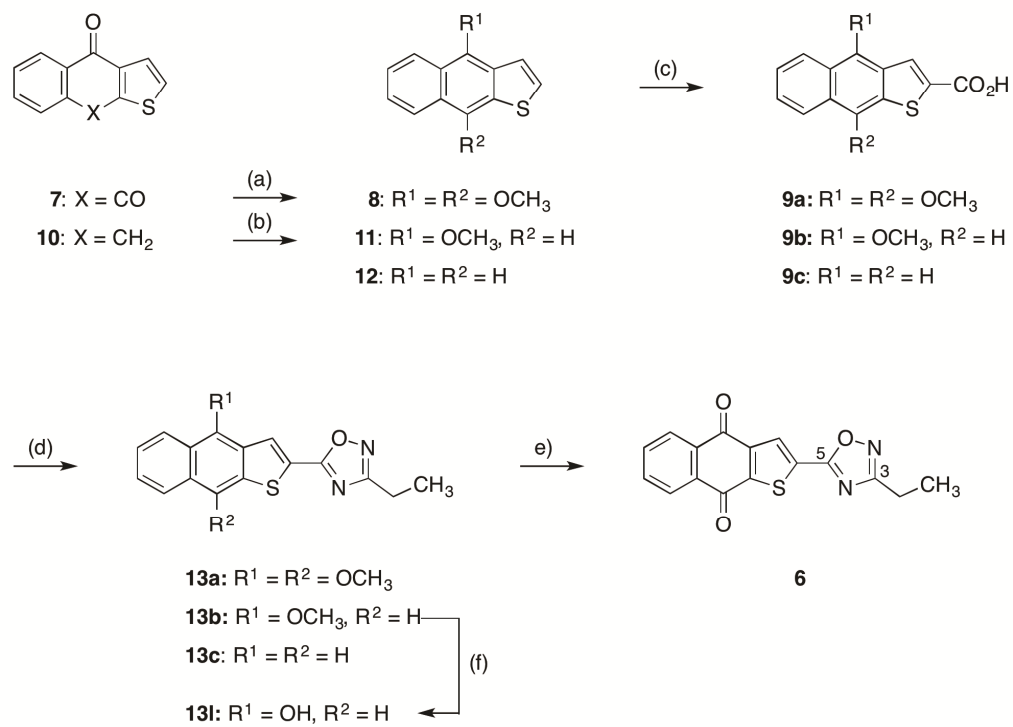
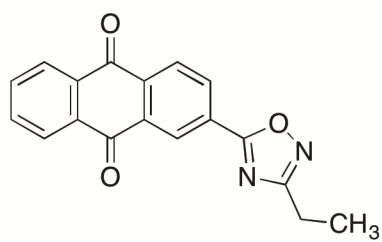
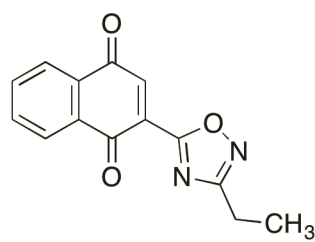
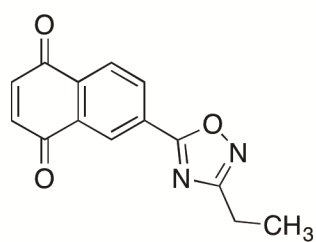
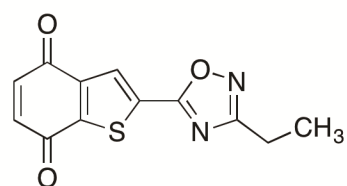


Chart 2

**13g** ($> 30 \mu\text{mol/L}$)**13h** ($> 30 \mu\text{mol/L}$)**13i** ($14 \mu\text{mol/L}$)**13k** ($11 \mu\text{mol/L}$)

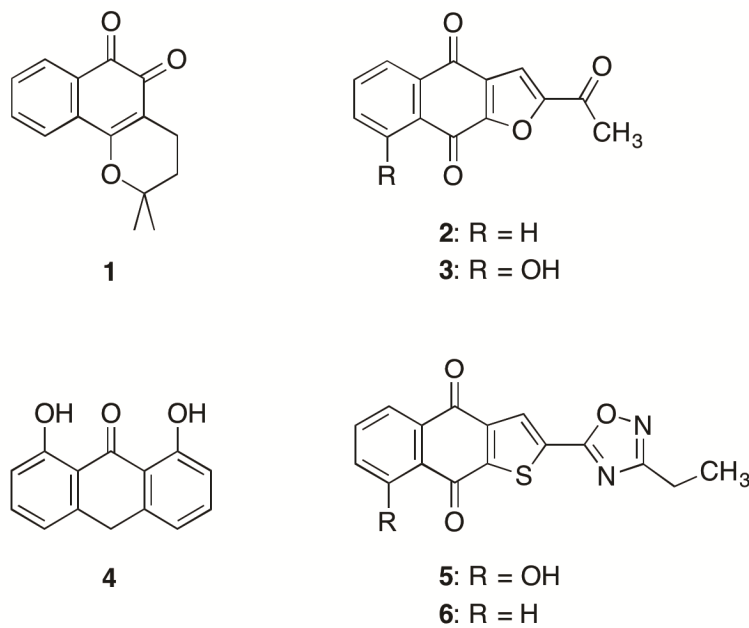


Figure 2

Scheme 2

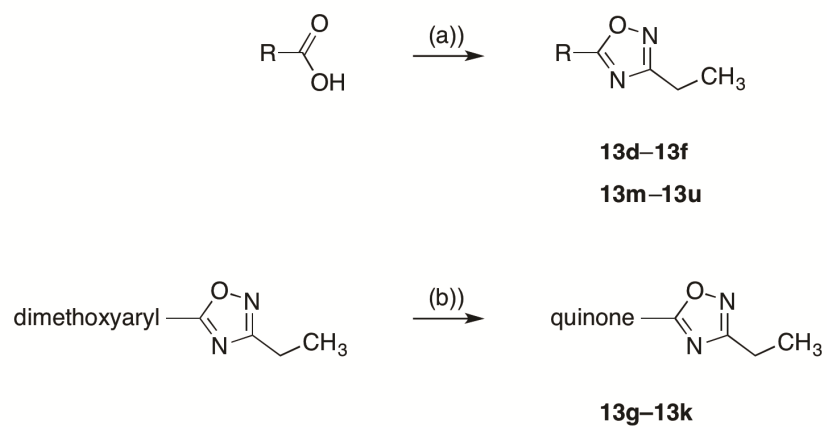
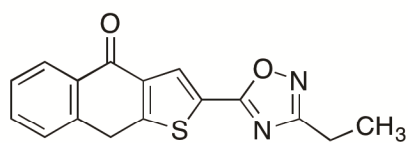
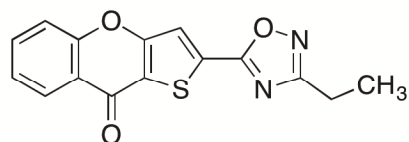
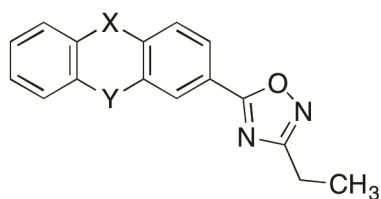
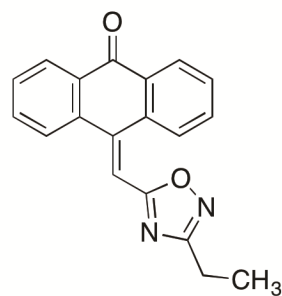


Chart 3

**13l** (7.3 $\mu\text{mol/L}$)**13m** (> 30 $\mu\text{mol/L}$)**13n**: X = S, Y = CO (> 30 $\mu\text{mol/L}$)**13o**: X = CO, Y = O (> 30 $\mu\text{mol/L}$)**13p** (6.5 $\mu\text{mol/L}$)

Scheme 3

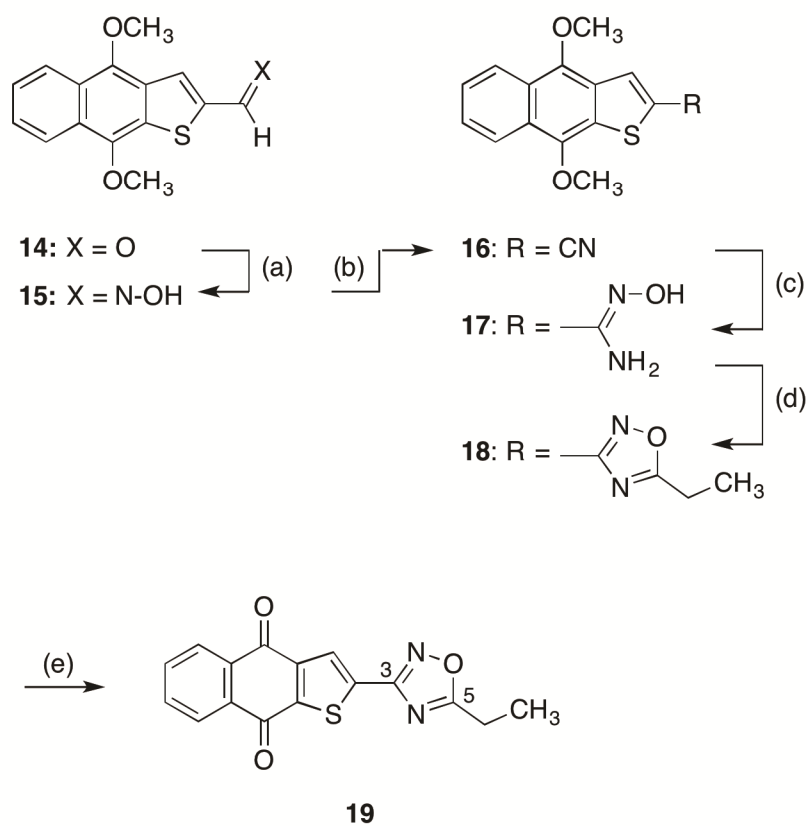
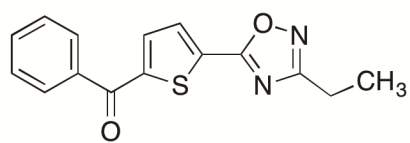
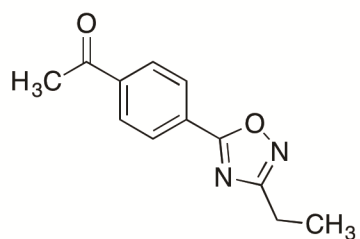
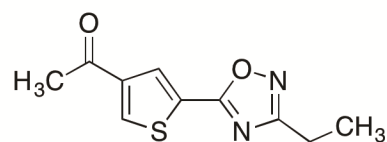
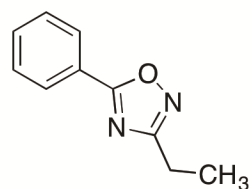
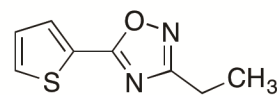
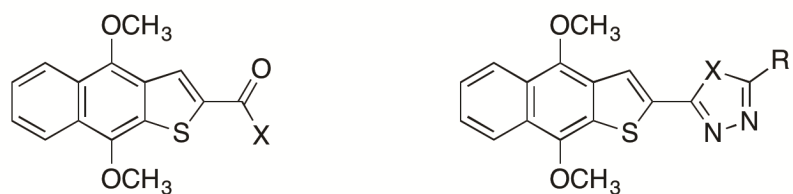


Chart 4

**13q** (> 30 $\mu\text{mol/L}$)**13r** (> 30 $\mu\text{mol/L}$)**13s** (> 30 $\mu\text{mol/L}$)**13t** (> 30 $\mu\text{mol/L}$)**13u** (> 30 $\mu\text{mol/L}$)

ACCEPTED

Scheme 4



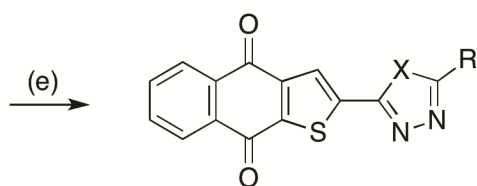
9a: X = OH (a)

20: X = OCH₃ (b)

21: X = NH-NH₂ (b)

(c) **22a:** X = O, R = H
22b: X = O, R = Me
22c: X = O, R = Et
22d: X = O, R = n-Bu
22e: X = O, R = Ph

(d) **23a:** X = S, R = H
23b: X = S, R = Me
23c: X = S, R = Et



24a: X = O, R = H

24b: X = O, R = Me

24c: X = O, R = Et

24d: X = O, R = n-Bu

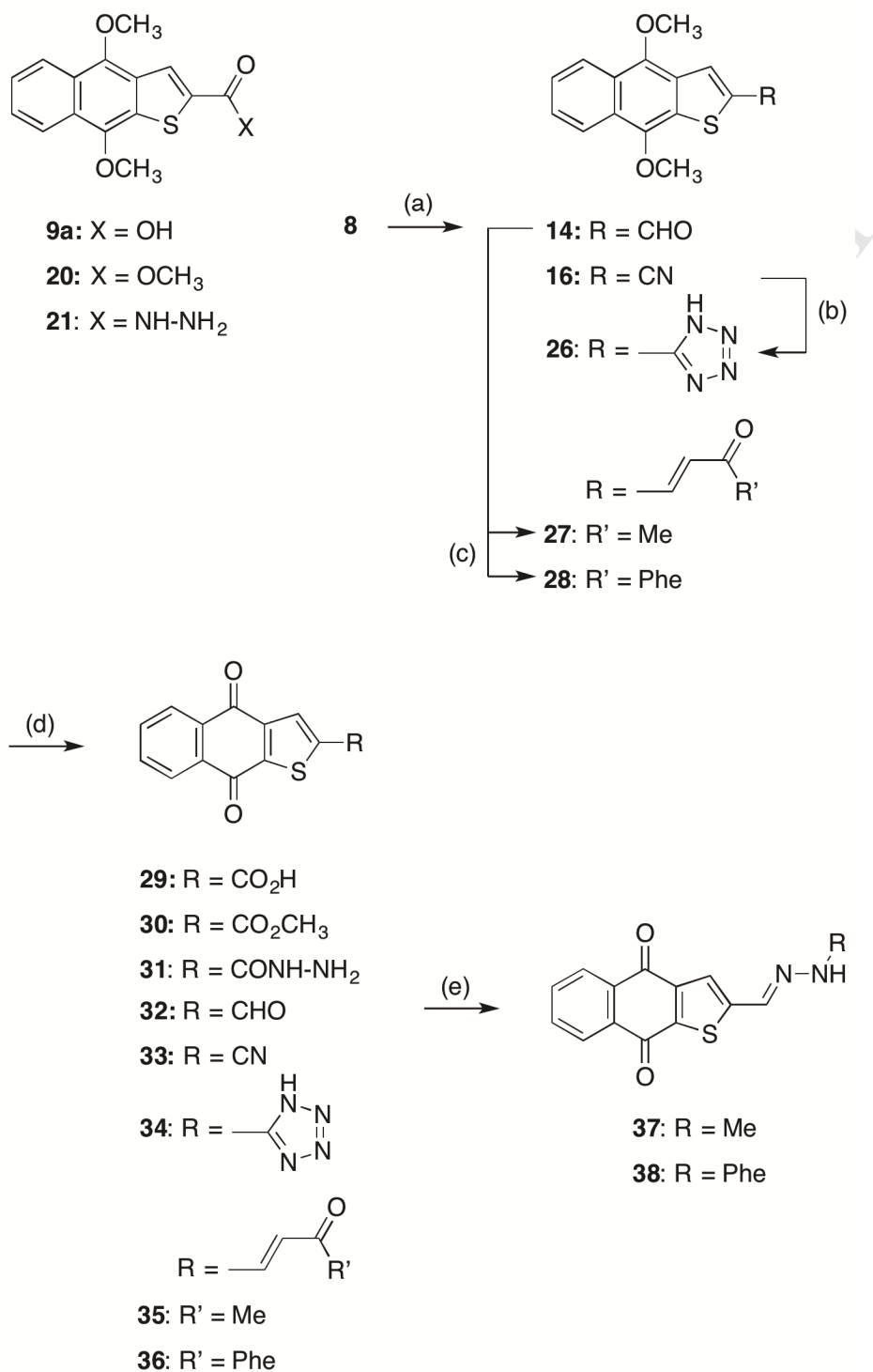
24e: X = O, R = Ph

25a: X = S, R = H

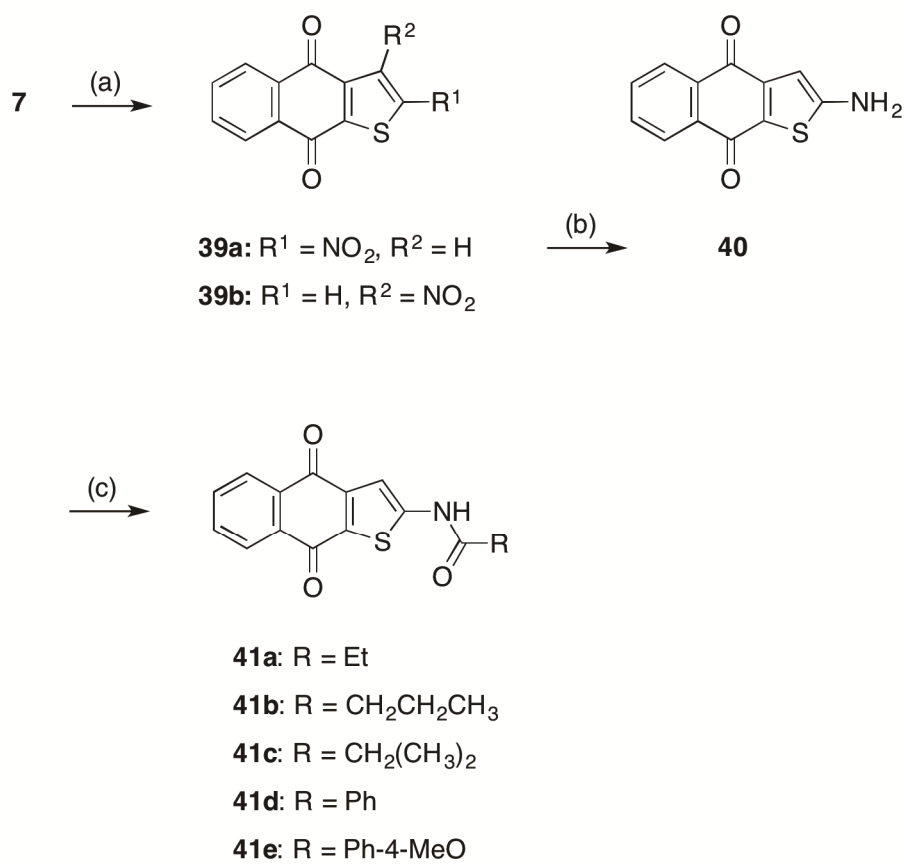
25b: X = S, R = Me

25c: X = S, R = Et

Scheme 5



Scheme 6



Highlights

- Novel analogues of oxadiazole-substituted naphtho[2,3-*b*]thiophene-4,9-diones were synthesized to define SAR for suppression of human keratinocyte hyperproliferation.
- The intact heterocycle-fused naphthoquinone was essential for potent suppression of human keratinocyte hyperproliferation, and an oxadiazole ring per se was not sufficient to elicit activity.
- Rearrangement of the heteroatom positions in the oxadiazole ring resulted in a highly potent inhibitor with an IC₅₀ in the nanomolar range.